AD NUMBER

AD867780

LIMITATION CHANGES

TO:

Approved for public release; distribution is unlimited.

FROM:

Distribution authorized to U.S. Gov't. agencies and their contractors; Critical Technology; MAR 1970. Other requests shall be referred to Air Force Rome Air Development Center, EMATA, Griffiss AFB, NY 13440. This document contains export-controlled technical data.

AUTHORITY

RADCAFSC, Itr 14 Oct 1971

RADC-TR-70-48
Final Technical Report
March 1970

7

10.6 MICRON OPTICAL SCANNER

Contractor: North American Rockwell Corp.
Autonetics Division
Contract Number: F30602-69-C-0136
Effective Date of Contract: 20 May 1969
Contract Expiration Date: 19 February 1970
Amount of Contract: $26,850
Program Code Number: HJ-05

Principal Investigator: R. L. Treuthart
Phone: 714-632-3614

Project Engineer: Robert F. Ogrodnik
Phone: 315-330-4305

Sponsored by
Advanced Research Projects Agency
ARPA Order No. 1279

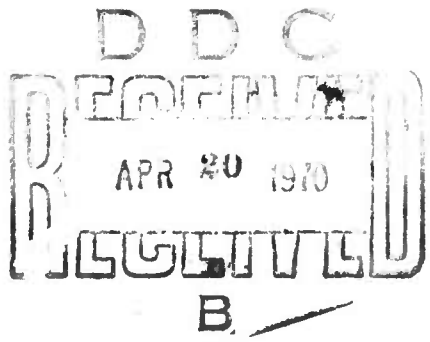

Rome Air Development Center
Air Force Systems Command
Griffiss Air Force Base, New York

51

When US Government drawings, specifications, or other data are used for any purpose other than a definitely related government procurement operation, the government thereby incurs no responsibility nor any obligation whatsoever; and the fact that the government may have formulated, furnished, or in any way supplied the said drawings, specifications, or other data is not to be regarded, by implication or otherwise, as in any manner licensing the holder or any other person or corporation, or conveying any rights or permission to manufacture, use, or sell any patented invention that may in any way be related thereto.

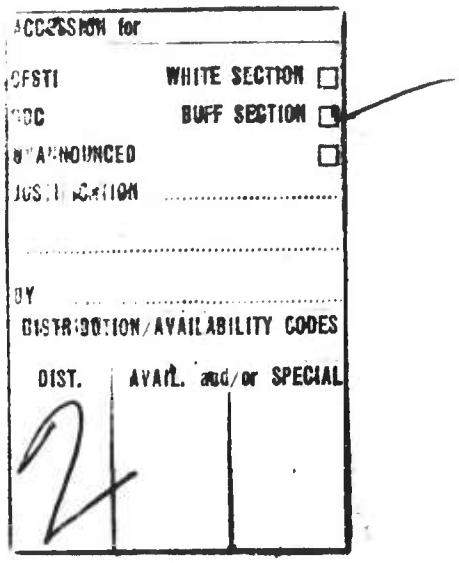

If this copy is not needed, return to RADC (EMATA), GAFB, NY 13440.

10.6 MICRON OPTICAL SCANNER

R. L. Treuthart

North American Rockwell Corporation

This research was supported by the Advanced Research Projects Agency of the Department of Defense and was monitored by Robert F. Ogrondnik, RADC (EMATA), GAFB, NY 13440 under Contract F30602–69–C–0136.

FOREWARD

This report was prepared by the Autonetics Division of North American Rockwell Corporation under Contract No. F30602-69-C-0136 issued by Rome Air Development Center, with Mr. R. Ogrodnik, EMATA, serving as program monitor.

This report covers work conducted from May 1969 to January 1970, and was submitted February 20, 1970. The principal investigator at Autonetics was Mr. R. L. Treuthart.

PUBLICATION REVIEW

This technical report has been reviewed and is approved.

Robert F. Ogrodnik
RADC Project Engineer

LEO W. SULLIVAN
Colonel, USAF
Chief, Surveillance & Control Division

ABSTRACT

A ballistic optical scanner stopped and reversed by a current impulse at each extreme of scan motion, and accomplishing each direction of scan motion via momentum from the drive impulses has been shown to be a feasible means of achieving equal observation times per scan resolution element. Operation from 0 to ± 3/4 deg mirror angle from 2 to 10 Hz has been shown to be feasible. Operation through this angle from 0 to 2 Hz in a servo mode, with the scanner displacement slaved to a triangular (or other) voltage waveform has also been shown feasible. This scanner, of 20 cm clear aperture at 45 deg incidence, has a versatility of control enabling a ballistic search mode to be stopped anywhere within one resolution element of scan ($\frac{1}{2}$ mrad mirror angle), where the position may be locked, or where target tracking may then be accomplished by the servo mode of control. The use of two independent mirrors will permit a raster scan having a 3 deg by 3 deg field angle.

CONTENTS

ILLUSTRATIONS

I. INTRODUCTION AND SUMMARY

In the field of laser radar, and more specifically for satellite ranging and tracking, there is need for a high resolution, large aperture, two-axis scanner providing a raster scan with equal observation times per scan resolution element. The feasibility of attaining these and further objectives has been conclusively demonstrated by the ballistic scanner feasibility demonstration model, which is the subject of this report.

In a complete system, the ballistic scanner would employ an azimuth mirror to generate a scan line of a raster pattern, with an identical elevation mirror to generate a step function between lines and to provide the retrace at the end of each raster.

We are now concerned with a single-axis feasibility demonstration model wherein a system of torquing coils distributed over the rear face of the mirror and to either side of the pivot axis is disposed within air gaps of an array of permanent magnets so that a current pulse in each of the coils produces a push-pull torque impulse on the mirror. The torquer structure is designed for optimal distribution of torquing impulse over the mirror to maximize torquing input and to minimize shock inputs resulting in mirror bending and acoustic mode patterns over the reflecting surface. This approach may be viewed in contrast to bending in a shaft driven mirror. Suitably sized impulses can accelerate, reverse, or stop mirror motion at any desired position. During time between reversals at each end of the scan line, the mirror is in an undamped, ballistic motion, that is, moving at a constant angular rate. This permits equal observation times per scan resolution element.

In addition to the ballistic mode of operation, a servoed mode is also employed. One function of the servoed mode is to lock the mirror in any desired rotational position. The mirror is displaced until its position pickoff signal matches a potentiometer reference voltage representing the desired null or lock position. Another function of the servoed mode is to slave the mirror position to an input voltage profile.

From 0 to about 2 Hz, the servo mode is effective in providing a linear scan, following an input triangular voltage waveform. Overlapping this rate and extending to 10 Hz, the ballistic mode provides a linear scan. Extension of this rate to 20 or more Hz is feasible. Toward 0 Hz the pure ballistic approach loses linearity because of the long line scan interval during which the effect of disturbing influences can become integrated. At the higher scan frequencies, the extreme power demands render feedback servo control impractical. However, although not attempted in the model, a combination of ballistic and servo control could be employed at the intermediate scan frequencies to further improve scan linearity.

Features and operational capabilities of a two-mirror ballistic scanner of the feasibility model type are listed below and have either been directly accomplished or have been proven feasible through operation of the model.

1. scan and step motions forming a raster pattern
2. interlaced scan
3. scan rates from 0 to 10 or 20 Hz
4. field angles from 0 to 3 or more deg
5. equal observation times per scan resolution element
6. scan linearity better than one resolution element
7. stopable within one resolution element (1 mrad of field)
8. switchable from large search field to small tracking pattern anywhere in search field
9. movable directly to any point in field
10. will slave to variety of scan profiles at low frequencies--triangular, sinusoidal, rectangular voltage waveforms
11. useful scan duty cycle of 90 percent at 10 Hz, approaching 100 percent at 0 Hz
12. large aperture (20 cm at 45 deg incidence)
13. analog or digital angle readout
14. computer controllable

II. DESCRIPTION OF MECHANICAL SYSTEM

General design and configuration of the scanner is given in figures 1 and 2 and is briefly described below.

The mirror subassembly is pivoted about an axis lying in the plane of the reflecting surface and includes a solid block of magnesium (AZ 31B-H24) which has been stress relieved at 300°F for 1 hour prior to nickel plating, polishing, and gold coating. It is substantially 9 inches wide parallel with the pivot axis, and 12 inches long, tapering in a series of slopes from 1.1 inch thickness at the center to 0.55 inch at the ends to minimize moment of inertia. On the tapered surface are a series of 8 grooved ridges extending the length of the mirror in planes normal to the pivot axis and serving as mountings for the rows of 120 sheet magnesium pylons which support a total of 15 planar torquing coils. The coils provide distributed torquing and are positioned by slots in the pylons to lie in planes parallel with the mirror pivot axis.

At the sides of the mirror are dovetail extensions to which the counterweight and pivot mount subassemblies are clamped to support the mirror. The counterweights are in the form of opposing pairs of Alnico V channel magnets encompassing stationary, pancake torquers. The counterweights are thus directly torqued, eliminating bending moments otherwise introduced in the mirror if the distributed torquer were required to drive the counterweights. On opposite faces of the torquer board through each counterweight is a pair of pancake coils, one coil serving to torque the counterweight, the other serving to detorque spring rate of the flexure pivots.

The mirror assembly and magnets for the distributed torquer are mounted within a frame consisting of side and end plates disposed on edge to form a box with open top and bottom. Beneath the mirror and bridging the space between sideplates of the box frame are 14 magnet mounting bars, each notched to receive 7 Alnico V magnets. A 15th bar supports soft iron

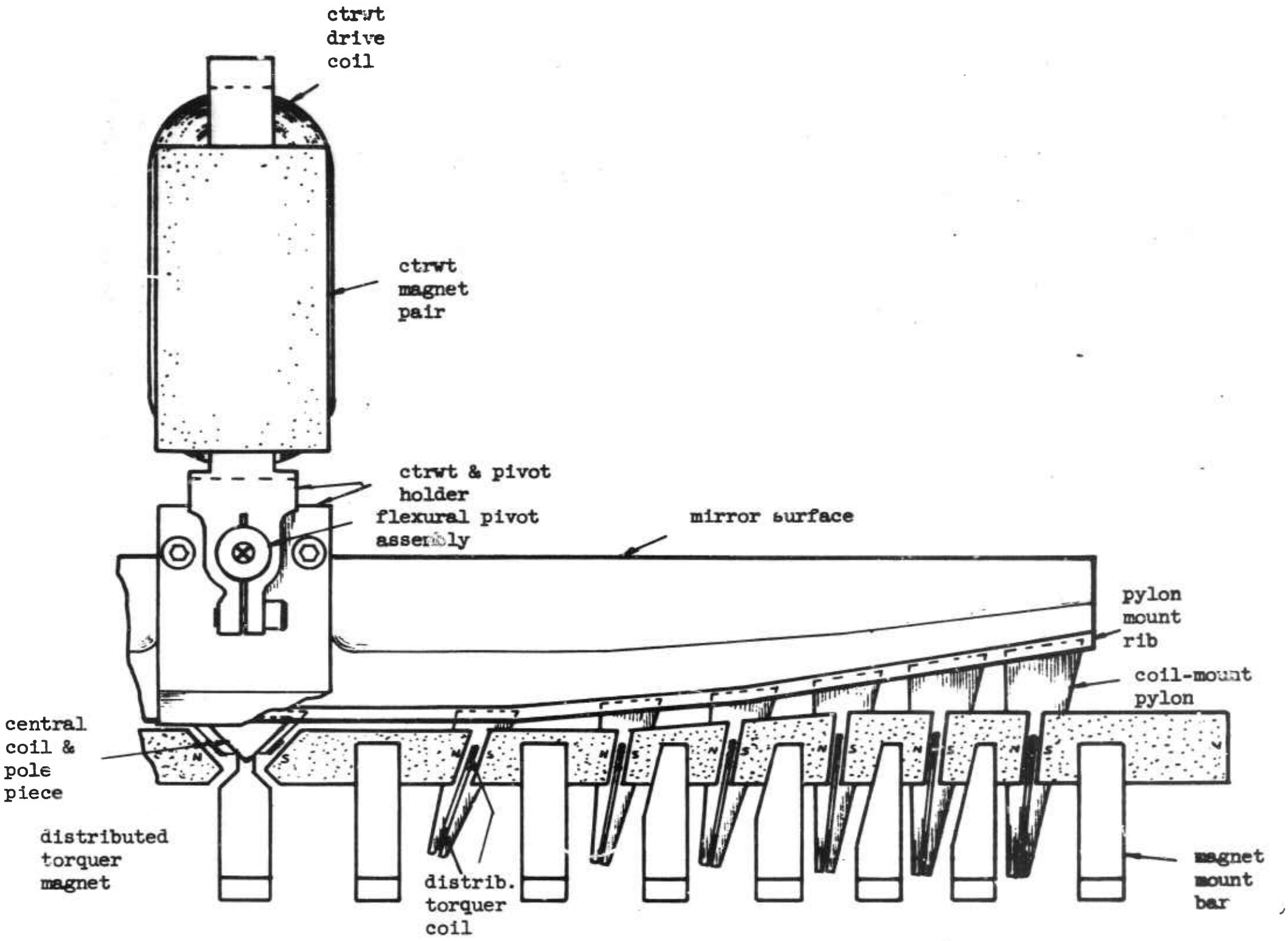

Figure 1. Mirror and Torquer Assembly

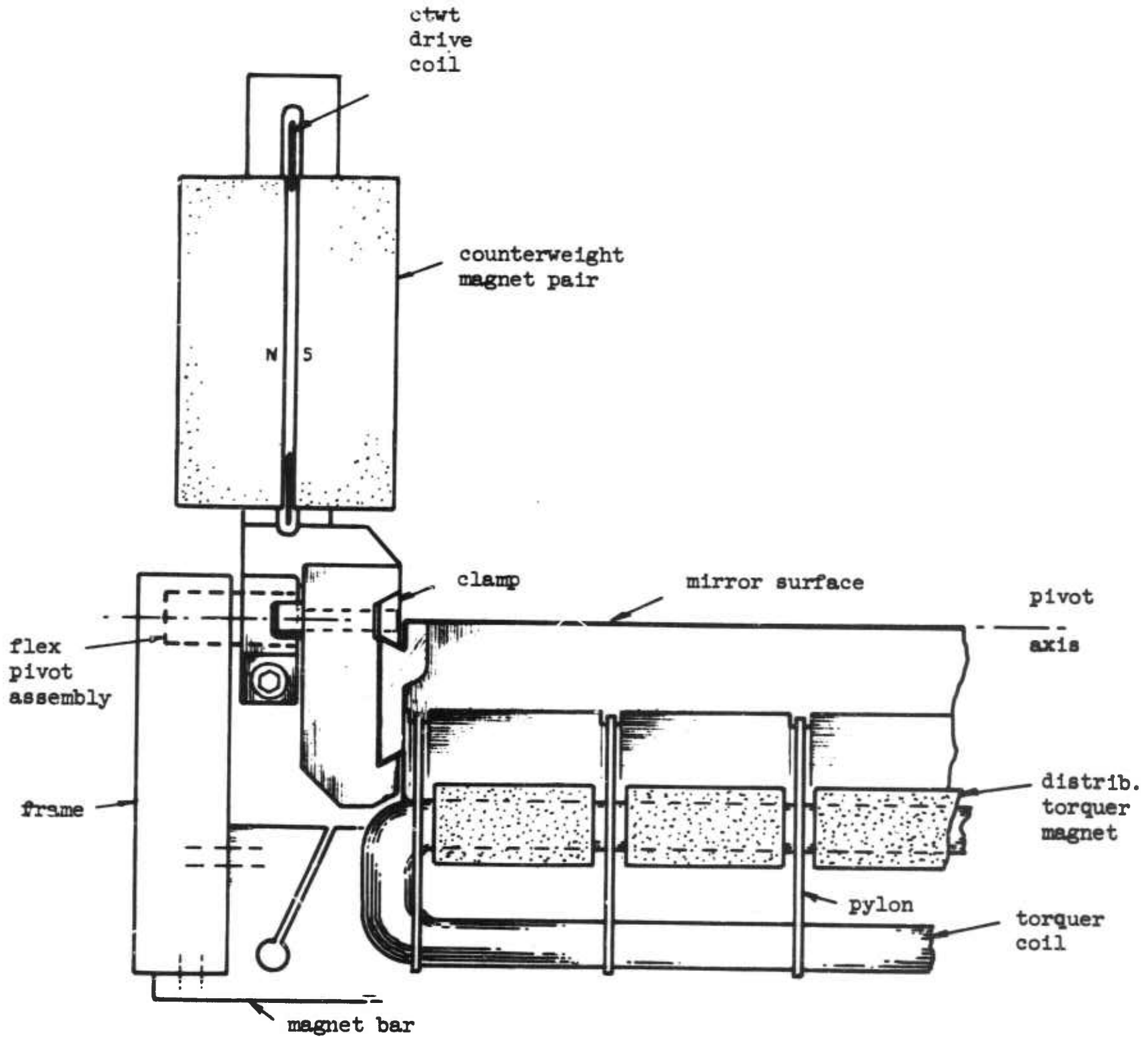

Figure 2. Mirror and Coil Assembly

pole pieces within the central drive coil; these are the only pole pieces employed. At the ends of the frame, limit stops are provided to prevent excessive mirror deflection, although in normal operation the stops will not be intercepted.

Magnets for the distributed torquer are of 0.4x1.03 inch and 0.53x1.03 inch cross section and of varying lengths. These are 96 in number and are each ground to form an appropriately sloped flux gap. The gaps are sloped to permit planes of the coils to pass through centers of percussion of the myriad of mass elements into which the mirror is imagined to be divided for purposes of design, and to pass through these centers normal to radii from the pivot axis to the centers. This arrangement affords maximum utilization of the torquing pulses and minimizes shock inputs to the mirror upon pulsing.

To monitor instantaneous displacement of the mirror, a position transducer of the linear differential transformer type is employed.* This is a cylindrical unit having a movable core within one primary and two secondary windings and is mounted from the box frame. At one corner of the mirror, the transducer core is positioned to move within the field structure along an arc of 6-inch radius. Core position in the dual secondaries determines the differential strength of the secondary output, which serves to produce a linear voltage ramp of magnitude representing magnitude of displacement, and of polarity representing sense of displacement. A 20 kHz excitation, becoming 40 kHz which is rejected in the rectifier circuit, permits readout of displacement at a time constant of response well below the transit time of one resolution element at 10 Hz for a 3-deg field of scan.

The pivot arrangement consists of crossed flexures accurately defining an axis of rotation and yet providing only 0.2 inch lb/rad each as a restoring torque.** Thus, bearing friction which would damp the mirror trajectory is avoided. The inconvenience of air bearings is also avoided.

---

*Tresco, Inc, Philadelphia, Pa; linear variable differential transformer, Model No. 65-00-100

**Bendix Corp., Fluid Power Div., Utica, NY; Cantilever flexural pivot, Model No. 5005-600, 5/32 dia.

The small spring rate is insufficient to delinearize the ballistic scan by more than a fraction of one resolution element of scan at 10 Hz, or 0.582 rad/sec. At lower scan rates. the effect of flexure stiffness on the ballistic scan can be cancelled by a fixed gain feedback from the position pickoff to the detorquing coils. However, at low scan rates it is feasible to slave the scanner to a triangular voltage waveform. Thus, the need for detorquing at low scan frequencies vanishes. If more sturdy flexures were employed, then at high and intermediate ballistic scan rates, flexure detorquing would be required.

Photographs of the scanner are shown in Figures 3, 4, and 5 with the test arrangement presented in Figure 6.

In Figure 3, illustrating the complete scanner, the mirror is shown within the box frame. Counterweight magnets are shown, with frame mounted yokes positioned to hold the counterweight torquer coils and the flexure detorquing coils. At the near corner of the scanner is the differential transformer pickoff, with the core mounted on the mirror. Adjustable, padded limit stops are shown at each end of the mirror. On the frame, a micrometer head is positioned to operate on a removable arm (not shown) extending from the mirror in order to check pickoff scale factor and linearity.

The flex pivots are mounted in arms shown attached to the side members of the frame. The mirror torquer current is supplied through these arms, which provide resilience against overconstraints along the pivot axis, which could damage the pivots. And more importantly, the arms are provided as a means of loosening as well as tightening the hold on the flex pivots. This permits adjustable shipping bars to be attached to the frame and mirror (at four tapped holes in the mirror) to support the mirror and yet remove load from the pivots during shipment of the scanner. With bars attached, the split arms are expanded, eliminating any restraint on the pivot assembly. (A more loadworthy substitute for the flexural pivot would be a pressurized air bearing. However, use of flexures appeared to be simpler for the feasibility model.)

Between the near end of the frame and the mirror can be seen seven torquer magnets. The magnets are also observed in the scanner underneath view of Figure 4, and are mounted on the transverse bars. Coils and support pylons for the distributed torquer are also observed.

In Figure 5, an inverted view of the mirror assembly is shown, where the pylons and torquer coils are displayed. Within the central coil are soft iron pole pieces. After assembly, these are made stationary and are not carried by the mirror. At the side can be seen the dovetail extension to which the counterweight and pivot assembly is clamped. The clamping is very localized, thus minimizing distortion of the mirror surface.

The test setup of Figure 6 shows the position pickoff electronics in the foreground, with the torquing electronics located immediately behind the scanner.

At the left of the scanner are power supplies for two polarities of voltage for the pickoff electronics, and a 20 kHz generator for pickoff excitation. Between this generator and the torquing electronics is shown a digital voltmeter used to calibrate the position pickoff. Behind this is a bias supply.

Behind the torquing electronics is an oscilloscope used to obtain test data given in this report. Finally, behind the scope is the torquing power supply on which is positioned a function generator to slew the scanner with a sine, triangle, or square voltage waveform.

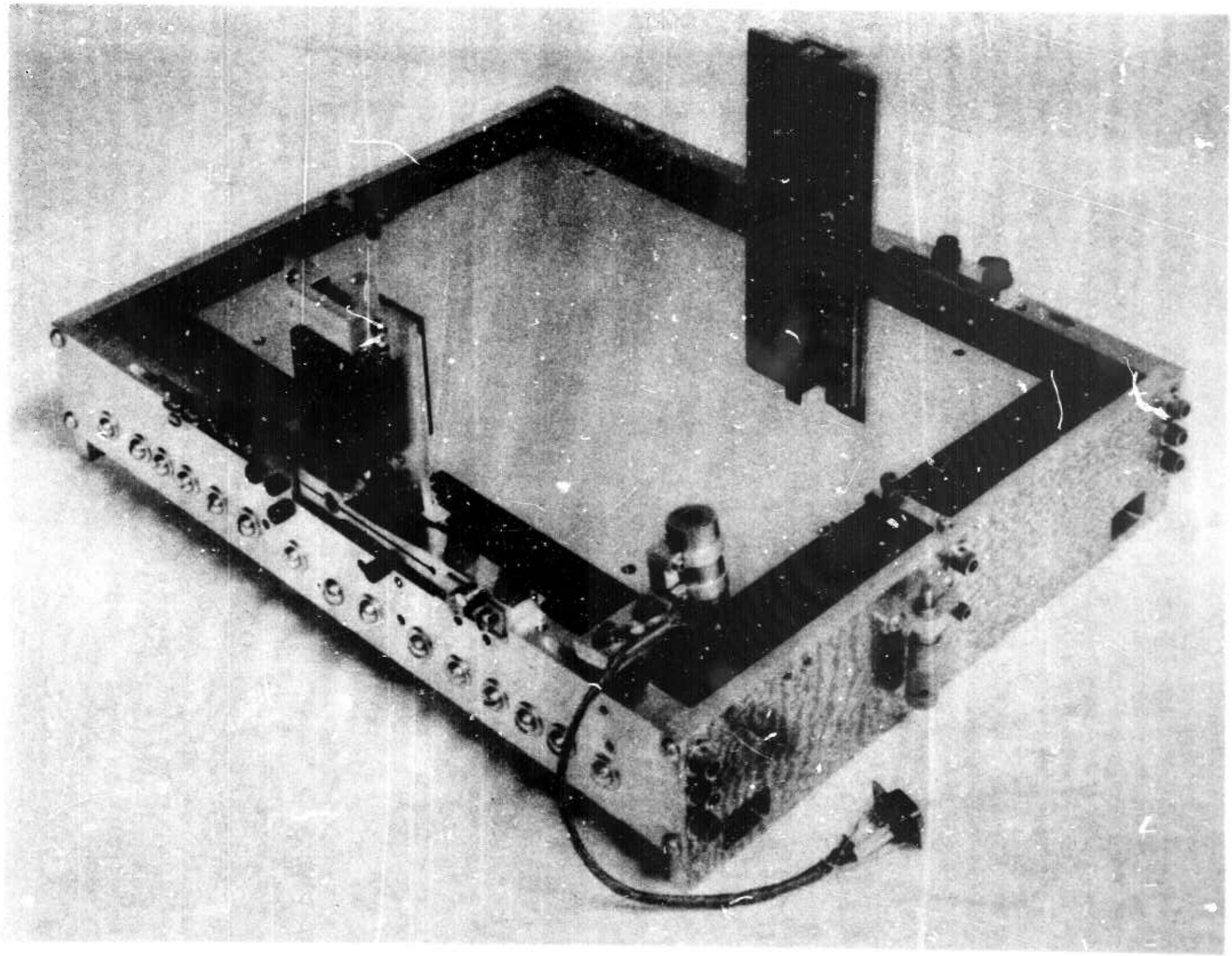

Figure 3. Ballistic Scanner Feasibility Model

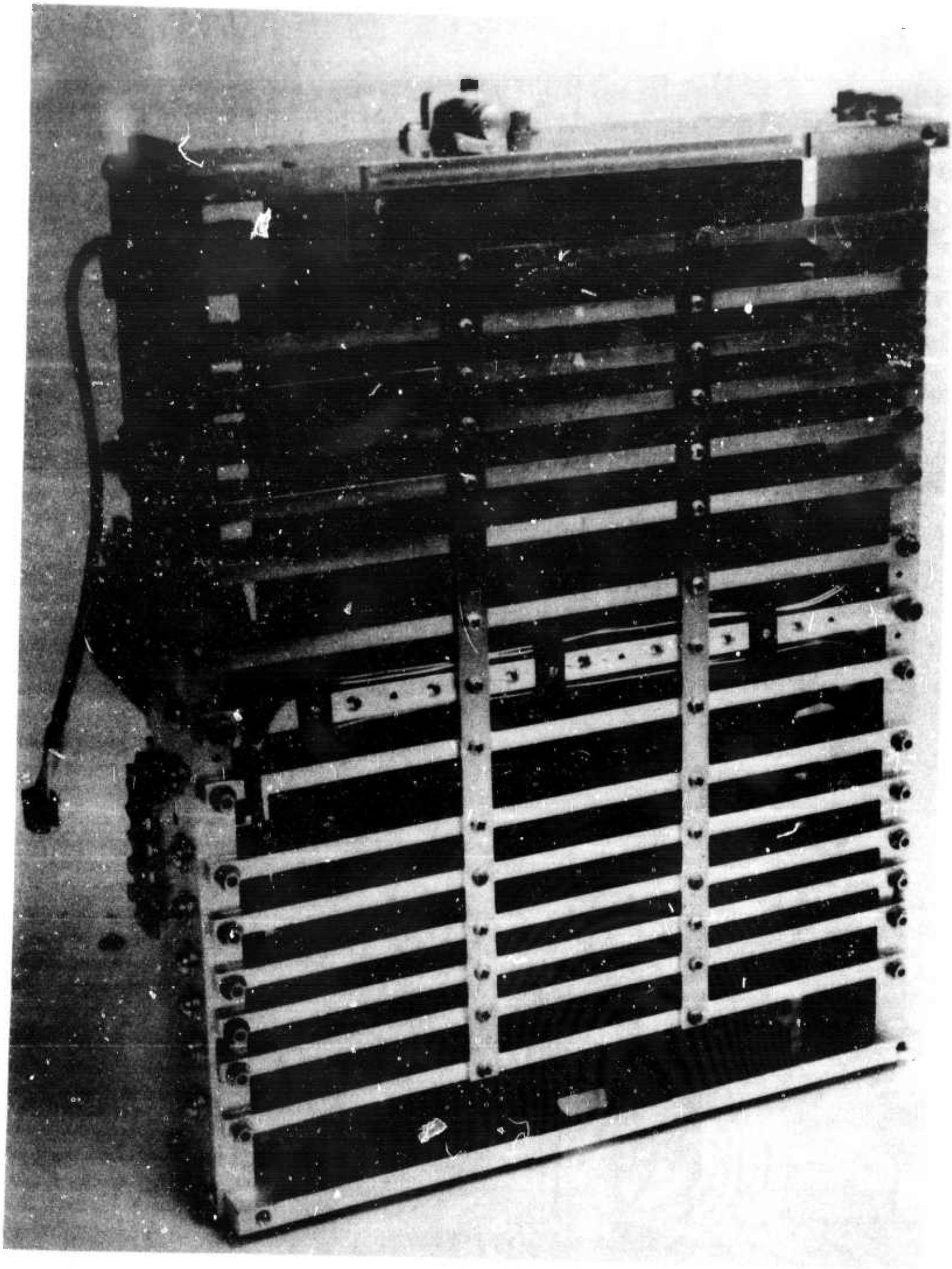

Figure 4. Bottom View of Scanner Model

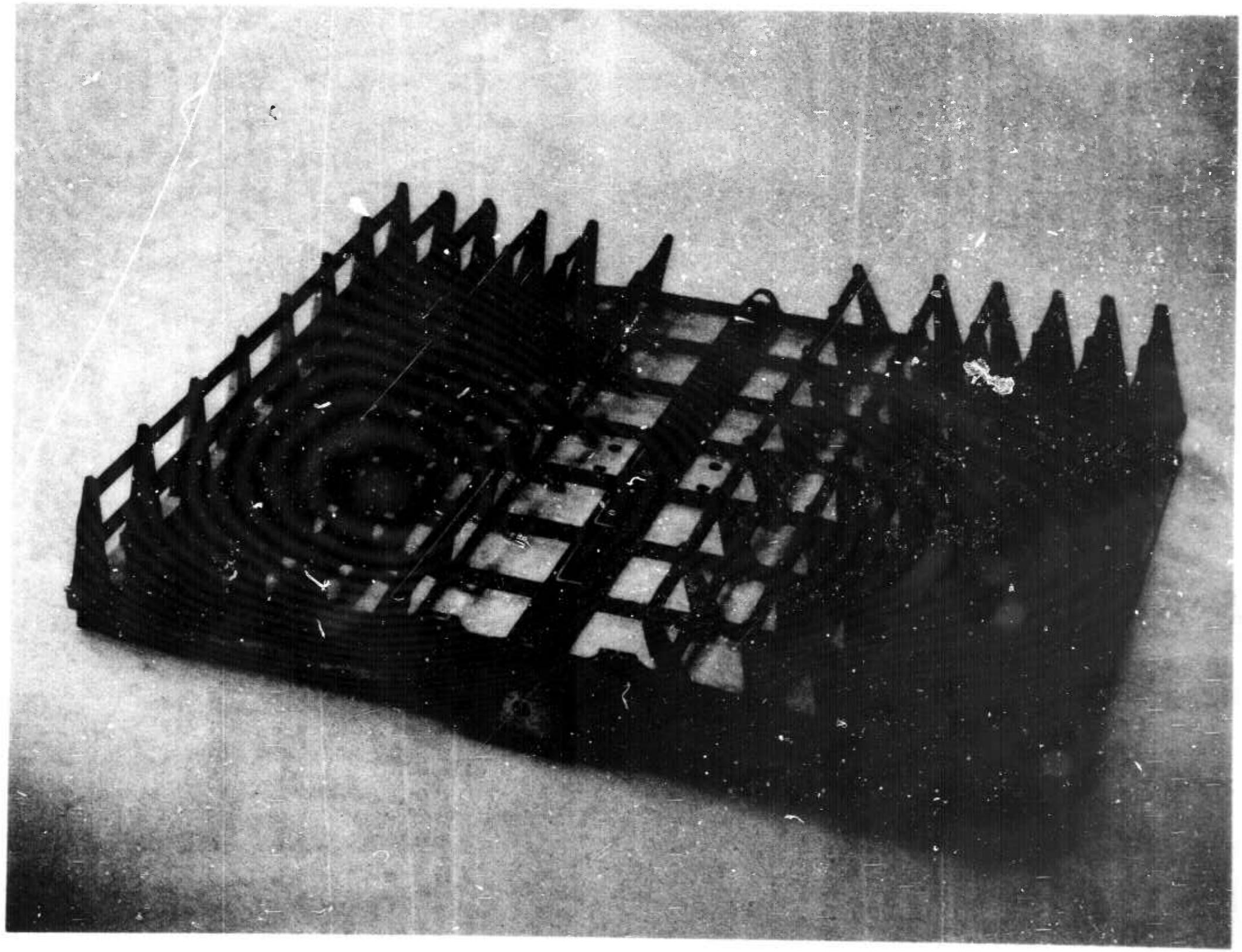

Figure 5. Mirror and Torquer Subassembly

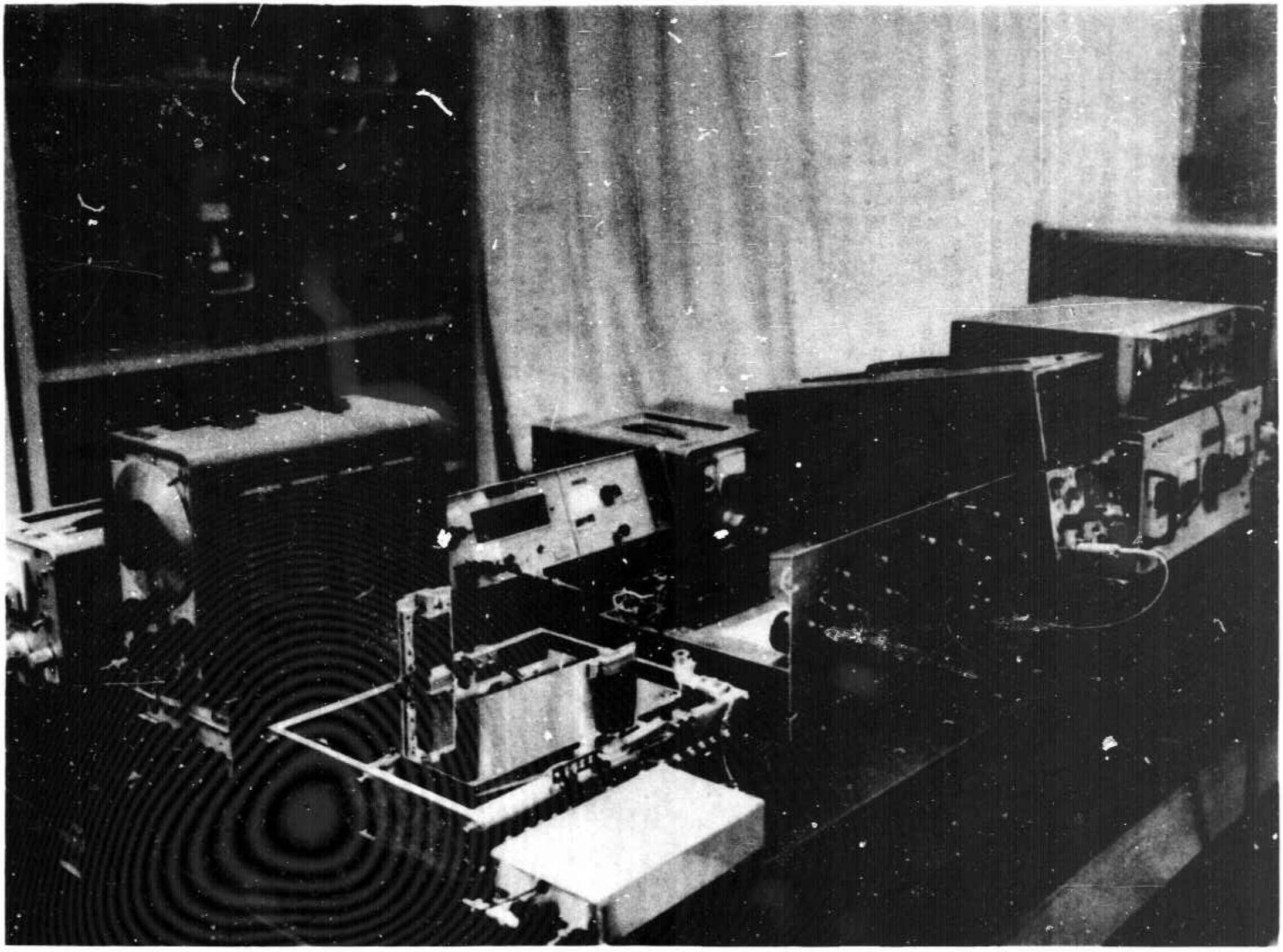

Figure 6. Scanner Test Arrangement

III. CIRCUITRY

Displacement Readout

In order to effectively control operation of the scanner, it was necessary to provide a displacement transducer and demodulator circuitry which could monitor an increment of displacement considerably less than the scan resolution element of $\frac{1}{2}$ mrad mirror angle, and with a linearity better than this angle. In addition, readout time constant must be considerably less than 1 msec, in view of a transit time of 0.86 msec for the scan resolution element when operating over 1.5 deg with a 0.9 scan duty cycle at 10 Hz.

These objectives are accomplished as follows. A linear variable differential transformer type of position transducer is operated at 20 kHz input, and the two outputs are each rectified by a full wave bridge, whose outputs are each routed through a stage of gain and isolation to a tuned filter rejecting 40 kHz but passing lower frequencies. The filter outputs are isolated by emitter follower stages and are summed. The differential signal is amplified by a 709 c I.C. gain stabilized amplifier. Response is 6 kEz at 3 db down.

Rudiments of the Torquing Circuitry

Two modes of operation have been incorporated in the scanner electronics, a ballistic mode and a servo or slave mode. Ballistic control is achieved by properly timed pulses of current in a forward or reverse manner to the distributed torquer and the counterweight torquer of the mirror. Servo control is achieved by slaving the mirror to the error signal between the position pickoff voltage and a control voltage, such as the triangle waveform of a function generator, a computer output, or a remote potentiometer whose setting can be employed to position the mirror or to lock it at a desired displacement.

In Figure 7, two power amplifier channels are used alternately to torque the mirror in a CW and CCW direction in response to inputs from a pulse generator via gate control circuitry. In the ballistic mode, excursion control circuitry permits manual setting of CW and CCW displacement limits of scan, giving out

a pulse from trigger circuits when the position readout voltage reaches these settings. Rectangular pulses thus produced are rounded off to reduce shock to the mirror and are directed through the appropriate power amplifier.

In the servo mode, the error signal obtained between the postion pickoff and either the slew generator or lock control is amplifified and directs positive or negative pulses, sampled from a 500 Hz clock rate, through the appropriate power amplifiers to the mirror torquer. An AGC circuit provides proportional control on the 500 Hz pulses. Pointing errors of about one tenth of a resolution element have been achieved.

Torquer Drive Circuit

Torquer drive circuitry is detailed in Figure 8. One requirement of the circuit is the need for reversal of current pulses in the torquer to reverse mirror motion. Another requirement is the change of impedance from a low value during pulse delivery to a high value between pulses to prevent counter emf during the ballistic scan from causing significant current to flow to damp the motion. Start, run, and stop torquing pulses are delivered by the same circuit, with the run pulses having twice the energy content of the others.

In the symmetrical circuit shown, a rectangular pulse applied to the CW silicon controlled rectifier (SCR) energizes the collector of the CW power transister. Then, a slightly delayed rounded current pulse derived from the same pulse that triggered the SCR is amplified and acts on the base of the power transistor, to pass current through the coil for CW torquing. For torquing in the CCW direction, the CCW SCR is actuated, and the CCW power amplifier passes a reverse current through the torquer. When no pulses enter the drive circuit the coil sees a high impedance at both transistors and SCRs. However, a 50 kΩ load is found necessary at each transistor, but this appears as a 100 kΩ load on the coil which keeps the current flow under the 1 or 2 volts counter emf negligibly small.

The counterweight torquers are now in series with the distributed torquer, but ideally, a separate drive stage as above would permit an optimum current ratio for the two torquers.

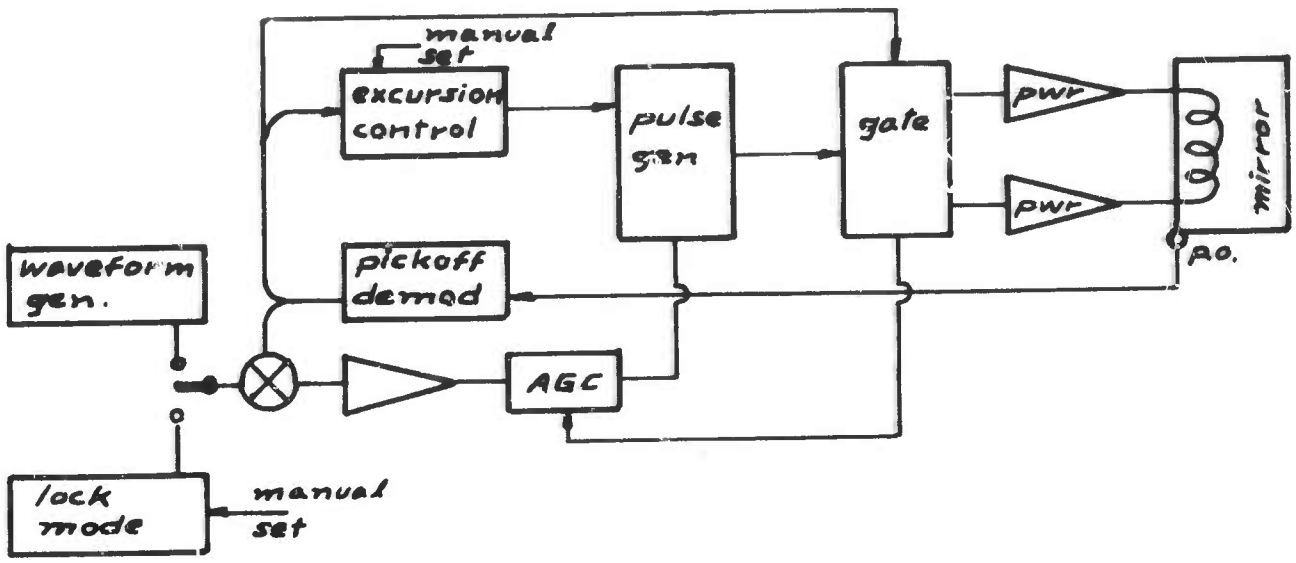

Figure 7. Scanner Simplified Block Diagram

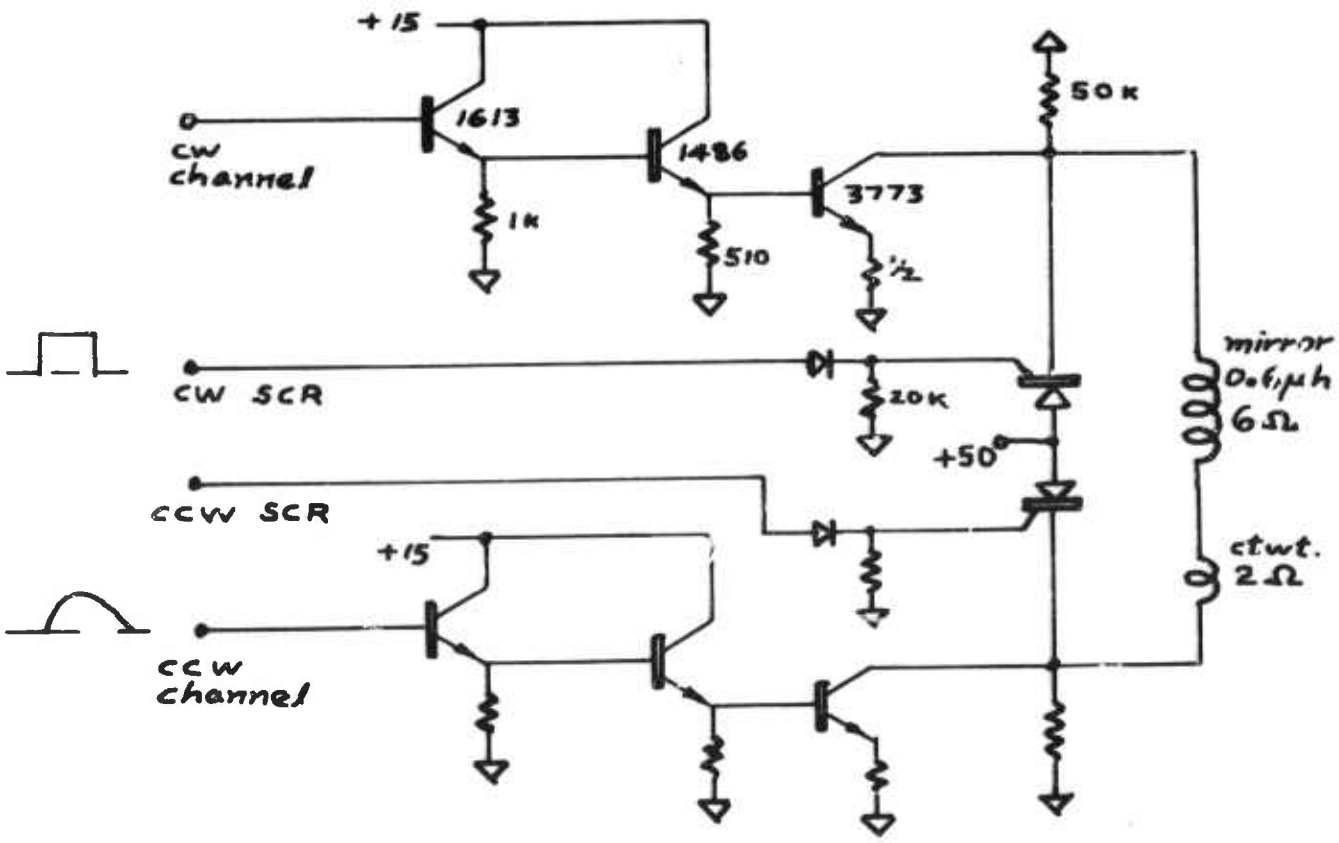

Figure 8. Torquer Drive Circuit

IV. SCAN CONSIDERATIONS

In order to more readily visualize the scan and stepping function contributing to generation of a raster pattern, reference is made to Figure 9. Angular position, velocity, and acceleration are shown for the scan and step functions. Accelerations are proportional to the pulse current and torque values.

It is observed that between useful scan intervals are short time intervals in which the scan is reversed by one mirror, and in which the raster pattern is simultaneously indexed to the next, oppositely directed, scan line by a second mirror. A return to the beginning of the raster pattern can be accomplished during the time of one scan line, where the second mirror is given a single scan simultaneously with a scan of the first mirror, effecting a diagonal retrace. Of course, other retrace programs are also feasible.

For the scan function, alternate and equal pulses are of opposite polarity to cause reversal of motion at each end of the scan line. Half height pulses are employed for startup and shutdown of the scan operation. For the stepping function, the current pulses are identical at each end of the scan line, since displacements of the mirror continue in the same direction prior to retrace. These current pulses are doublets, consisting of equal forward and reverse polarities, first accelerating the mirror and then immediately bringing it exactly to rest.

With two independently controllable axes of scan, each with a ballistic and servo capability, great versatility of scan pattern is available. For illustration only, versatility of control is shown in Figure 10; these scan functions are feasible, but no assertion is made that all are optimal or even desirable.

Assume the scanner is commanded to scan in a raster pattern as in Figure 10(a). When target T is intercepted, the large raster may be switched to the small raster of Figure 10(b) to increase the frequency of

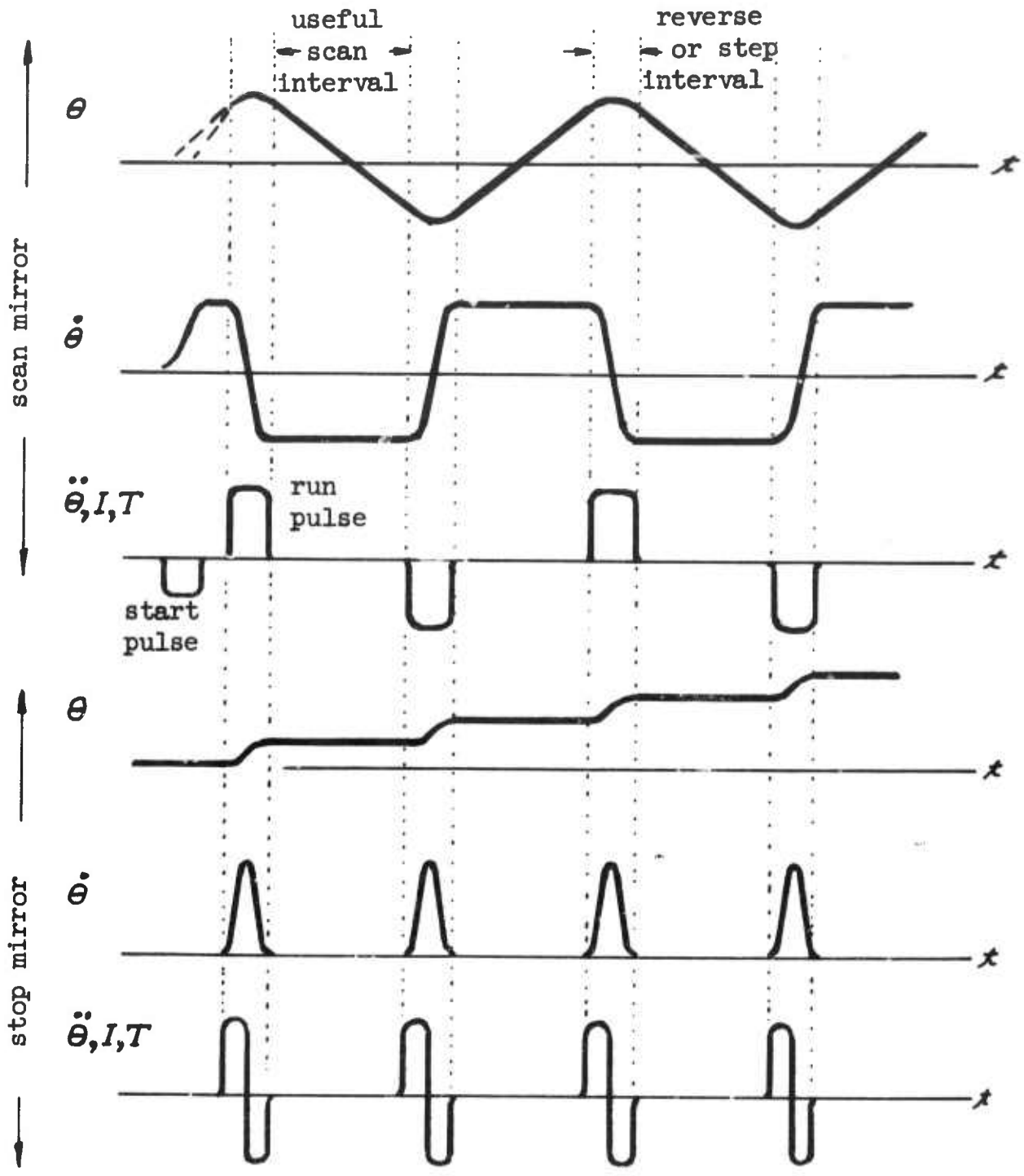

Figure 9. Scan Parameters

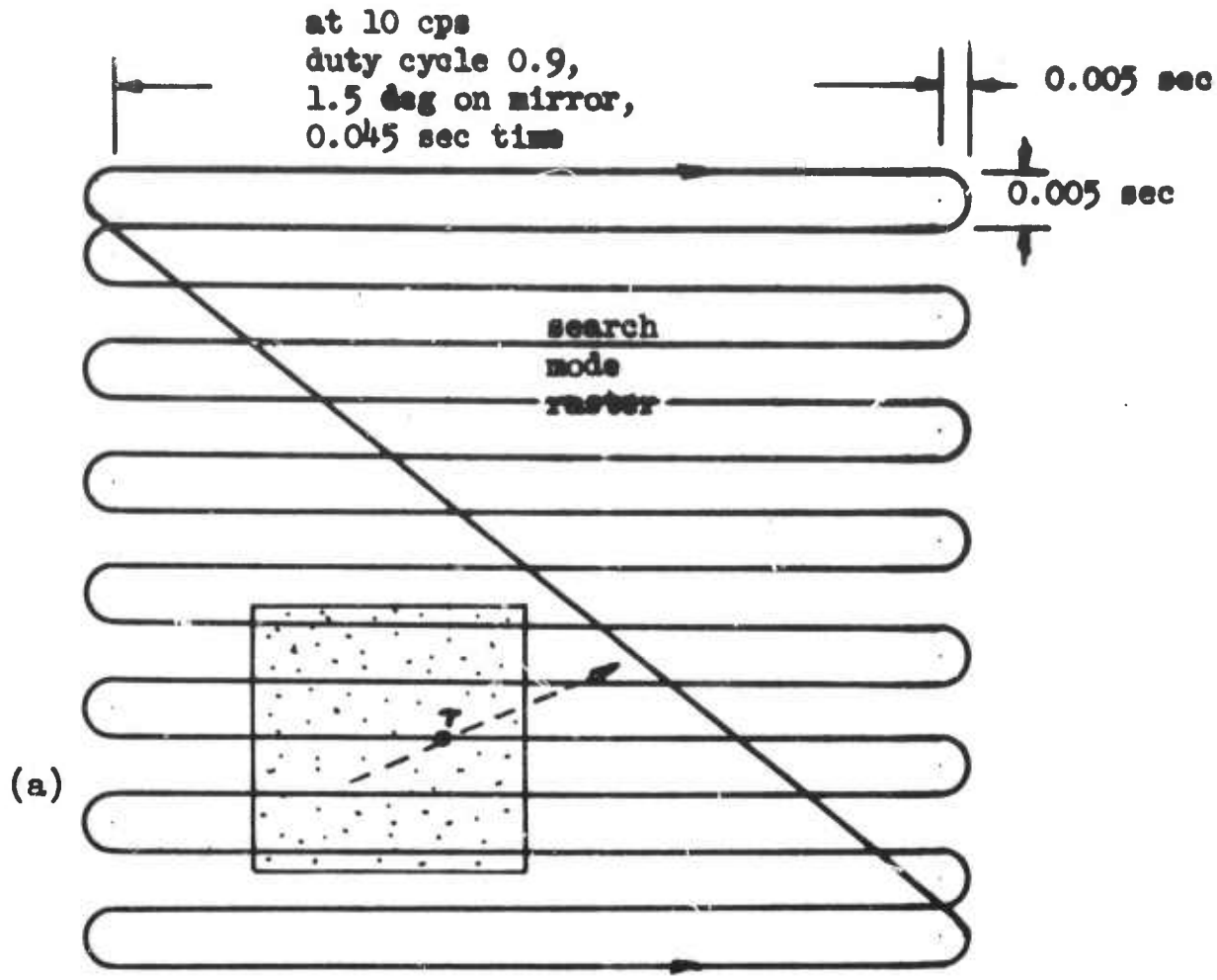

Figure 10. Scan Patterns

target crossings, obtaining more information to improve position determination. Or, the interlaced scan of Figure 10(c) might be employed. The shaded area within the large search raster indicates the initial position of the reduced raster, which may represent a reduced field of search or else a tracking raster. This can be swept by the scanner servo control within the boundaries assigned the large raster to encompass the target in its trajectory. The reduced raster may be either ballistic or servoed, and is either superimposed on a servoed slew, or the line reversals are updated to simulate a raster slew.

If the target trajectory is unknown, a computer can utilize target returns to quickly determine a trajectory and further modify and shrink the raster for optimum tracking. As target tracking becomes updated, the track pattern may be substantially eliminated with scanner servo control on each axis commanded to precisely follow the target.

However, with prior knowledge of target trajectory in the computer, the first target pickup may command the scanner to go directly from a large raster to a precision track mode, although a quickly reduced track pattern as in 10(d) may be preferred to better achieve transition from search to target track mode and final clamping on target. The latter pattern is shown as a spiral, that is, a travelling circular scan having many target crossings and decreasing in amplitude as target clamping improves. This is achievable by switching from the ballistic search mode to a servoed track mode with sinusoidal voltage inputs 90 deg out of phase between the two mirrors.

For a 10 Hz ballistic line scan of 0.9 duty cycle, 1.5 deg or 0.045 sec time, we have a scan reversal in 5 msec, requiring an acceleration α over 2.5 msec of 232 rad/sec^2 for a rectangular torquing current pulse. For illustration, if we assume the same torquing capability to be available for a servoed circular tracking scan where each mirror wobbles with, say, an amplitude θ of $\pm$ 1.25 mrad, the frequency of the resultant conical scan of 5 mrad field angle can be obtained as follows.

$$\theta = \theta_o \sin \omega t$$

$$\ddot{\theta} = -\omega^2 \theta_o \sin \omega t$$

$$\frac{\ddot{\theta}}{\omega^2} = -\theta_o \sin \omega t$$

Adding the first and second equation,

$$\frac{\ddot{\theta}}{\omega^2} + \theta = 0$$

or $$\omega = \sqrt{\frac{\ddot{\theta}}{-\theta}}$$

From the third equation we find angle is negative when acceleration is positive. Thus,

$$\omega = \sqrt{\frac{232 \text{ rad/sec}^2}{-(-1.25 \times 10^{-3} \text{ rad})}} = 431 \text{ rad/sec}$$

$$f = \omega/2\pi = 68.6 \text{ Hz}$$

Thus, it is seen that substantial frequencies are possible for small tracking angles, provided we are willing to meet the servo amplifier requirements. For more modest amplifier requirements, lower conical scan rates will be realized, where frequency varies with the square root of acceleration and hence of the current value.

We may presume that maximum utilization of the scanner requires the two-mirror assembly to be mounted on gimbals which provide course pointing and track rates. Irregular motion of the gimbals within angular limits smaller than the scanner field of view, as the gimbals attempt to match the target rate readout by the scanner, can be accommodated by resilience of the scan achieved through optimal combination of ballistic and servo controlled scanner drive inputs, thus keeping the scanner on target. Resilience is achieved by versatility of scan pattern and the ability to slew a small pattern within the boundaries of the large pattern which represents displacement limits of the scanner.

V. TEST RESULTS

The performance of the scanner as of the time of this writing can be reported no more realistically than by a presentation of oscilloscope photographs, for which descriptions are given below. Position readout linearity data and mirror flatness are also described. Performance capability that may be extrapolated from these results is discussed in Appendix I.

Servo Scan Mode

Figures 11 through 18 represent the servoed mode of scan, wherein the scanner is slaved to the error signal developed between its position pickoff voltage and the waveform voltage of a function generator. In evaluating these figures, it is to be noted that a peak-to-peak voltage of 12.48V represents 1.5 deg of mirror motion, based upon the particular scale factor of the pickoff electronics during these experiments. (This scale factor depends upon amplitude setting of the 20 kHz pickoff excitation generator which is put at approximately 6V rms.) The oscilloscope in all cases monitors the position pickoff DC voltage from the pickoff demodulator circuit.

Figure 11 - This is a $\frac{1}{2}$ Hz triangular scan of 1.5 deg, and is quite linear.

Figure 12 - This is a 1 Hz triangular scan of 1.5 deg showing overshoot at the reversal of motion in each direction. This is because of the need for more gain on the differentiated pickoff signal to command extra current for sharper scan reversal. However, only enough gain is required during the straight portion of the scan to establish the scan rate and to thereafter overcome any small damping or spring rate. After all, the mirror will coast at one velocity or another without any servo gain.

Figure 13 - A 2 Hz triangular scan of 1.5 deg is shown. Servo amplifier gains have been increased. The gain at reversal is still inadequate; and in attempting to make up for this, gain during the straight line scan has been left higher than desired, providing a slightly erratic trace.

Figure 14 - An expanded trace of Figure 12 shows what may be a 60 Hz ripple upon which is the approximately 500 Hz control frequency. Or, this may be an advance of the mirror due to the small pulses, followed by a retardation as the small pulses reverse. The ~ 60 Hz component has a displacement of about 60 mv from the average scan trace, representing roughly $\frac{1}{2}$ percent ripple. The 500 Hz pulses of about 40 mv to either side of the 60 Hz ripple represent about a 1/3 percent disturbance, based on the 12.4 volt full scan of Figure 12. It is seen that 3 or 4 torquing pulses of alternating polarities control the scan. Which part of the 500 Hz ripple can be viewed as coupling in the electronics and which part as jitter of the mirror has not been determined but it is probably largely on the mirror, which brings up the question of mirror dynamic flatness. When proportional control is put in operation, these pulses will be virtually absent during the straight part of the triangular scan where the mirror is coasting and requires guidance, not propulsion.

It remains that the only significant nonlinearity of trace is at scan reversal, where more gain is needed. However, if the scan duty cycle is reduced from unity as shown in these oscillograms to about 0.8, the overshoot will be outside of the useful range. With more effort, there is no reason why this linear duty cycle range cannot be extended to 0.95 or better for the servoed mode at 2 Hz; and of course, the linear range improves at lower scan frequencies.

Figure 15 - Here is a $\frac{1}{2}$ Hz sinusoidal scan of 1.5 deg. Especially at the top of the trace, one can see the 60 Hz component observed in Figure 14. Waveform distortion observed at the top of the sinusoid may indicate nonuniform flux at the torquer but can be cured by higher servo gain.

Figure 16 - This is a 1 Hz sinusoidal scan.

Figure 17 - Here is a scan resulting from a $\frac{1}{2}$ Hz square drive function. With improved gain and feedback control, a much improved scan would result, although a square scan was not an objective of this development effort.

Figure 18 - Here the scanner is in the lock mode, which can be set at any voltage level within ± 6.2 volts to place the angular position of the mirror as desired. After the trace proceeds, a 10 gm weight is added to the mirror at 6-inch radius, causing a change of position in order to

increase the error signal. The position change is less than the ½ mrad (or 0.24V) mirror angle resolution element sought.

Ballistic Scan Mode

Figures 19 through 24 represent the ballistic mode of scanner operation; other conditions remaining as before.

Figure 19 - Here, a 4.6 Hz scan rate is employed. Appreciating that the scan amplitude is controlled by giving a reversal pulse to the mirror torquer when it reaches the desired displacement, threshold levels of the Schmidt triggers which monitor the pickoff output are set to the upper and lower voltage values shown on the oscillogram. These levels represent a 1.5 deg peak-to-peak scan. Then, the drive current is turned up, and the 4.6 cps scan results. There is a shortage of drive current, for reasons explained elsewhere.

Figure 20 - In this oscillogram a 10 Hz scan is observed. Here, the drive current was put at maximum and the Schmidt trigger thresholds were lowered to shorten the CW and CCW scans so that 20 ballistic transits could be made in 1 sec, giving 10 Hz operation.

Application of torquing can be noted at peaks of the trace. Discounting these intervals, we have a useful scan from +2.7V to -2.5V, giving 5.2/12.4 = 0.42 times the displacement sought. As before, torquer current is inadequate and is the only reason that 10 cps at full displacement (1.5 deg or 12.4 volts) was not reached.

Figure 21 - Although the current has apparently been reduced, giving only 3.7 Hz, this oscillogram is essentially an expansion of the 4.6 Hz trace of Figure 19. In fitting a straight line (taut thread) to the expanded trace, a slight slowing, or rightward bending, of the trace is noted just before the bottom reversal, and in smaller amount, a slight acceleration is noted just after the upper reversal. This is because the flexural pivot stiffness has not been detorqued. The detorquing coils are incorporated, but no detorquing amplifiers have been fabricated.

The lower offset, measured vertically to find the voltage error just before the reversal pulse, is about 1 mm or 0.2V, representing a scan nonlinearity of 0.2/12 or 1.6 percent.

A small ripple is noted on the trace. This seems to be in the very general neighborhood of 100 cps, and evidently represents a mirror flexural resonance due to the excitation impact from the 5 msec torquing pulse. Its affect on dynamic flatness of the mirror is not known.

Figure 22 - This oscillogram is essentially an expansion of the 10 Hz trace of Figure 18, although taken at a different time. The frequency is substantially 10 Hz, except that the long down slope shown is slower than the upward one to the right, due to walkoff, thus appearing equivalent to 8.3 Hz. The ripple shown in Figure 22 is considerably reduced below that of Figure 20 and provides no further insight on the ripple of the latter trace, as had been hoped.

Figure 23 - The scanner is observed to work well to 1 Hz or a little lower. At $\frac{1}{2}$ Hz at full amplitude the spring rate discourages continued operation, causing the slow displacement to be arrested short of reversal thresholds. If detorquing of the flexure pivots were employed, operation would be satisfactory at even lower rates. However, the alternate servo operation makes that unnecessary.

Figure 24 - Here is a 2 Hz ballistic scan of 1.5 deg displacement. A slight ripple is detectable, and the effect of spring rate can, with difficulty, be observed on the approach to the lower scan reversal.

Position Readout Linearity

Position readout linearity is required to be within one resolution element of scan, or $\frac{1}{2}$ mrad on the mirror. Linearity has been shown to be within $\frac{1}{4}$ mrad or one percent of the peak to peak scan.

Mirror Flatness

Mirror flatness was desired to be one-tenth wave at 10 microns wavelength. This condition was met before assembly. After addition of the torquer and counterweight assembly, a test was made with a 6-inch optical flat resting over lens tissue on the mirror. Flatness was found to be 0.16λ at 10 microns with the scanner at ambient temperature. After one half hour of operation of the scanner in the servo mode at half displacement at 1 to 2 Hz, flatness improved slightly. The fringe test pattern is portrayed in Figure 25.

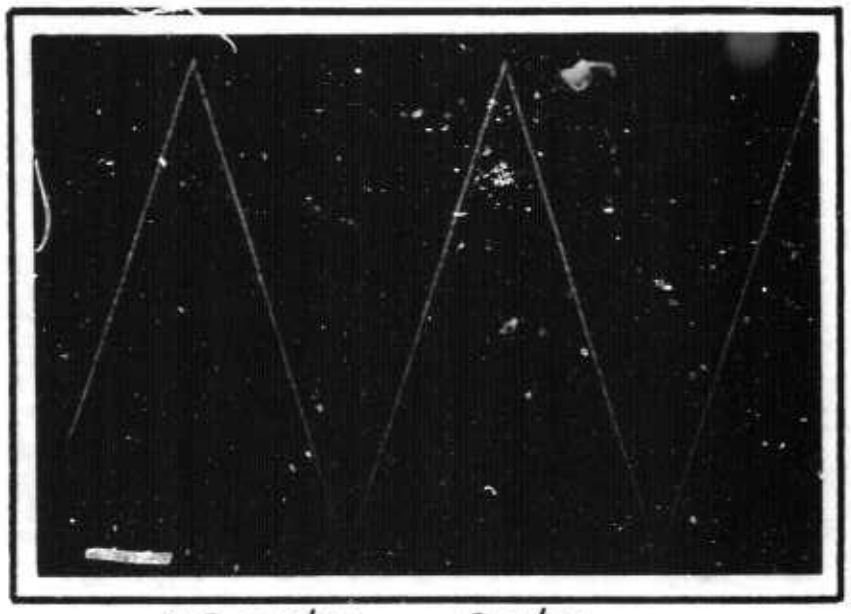

0.5 sec/cm 2 v/cm
Figure 11. Triangle Scan, $\frac{1}{2}$ Hz

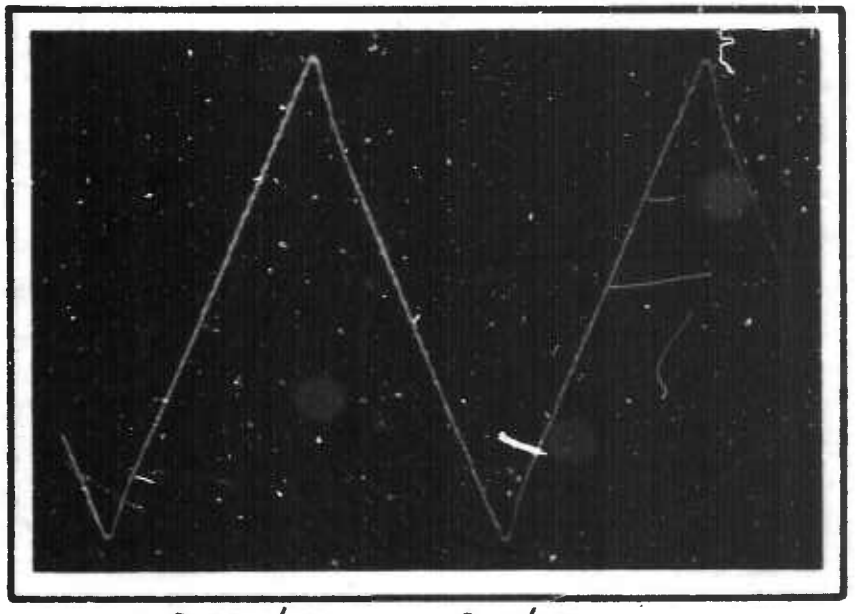

0.2 sec/cm 2 v/cm
Figure 12. Triangle Scan, 1 Hz

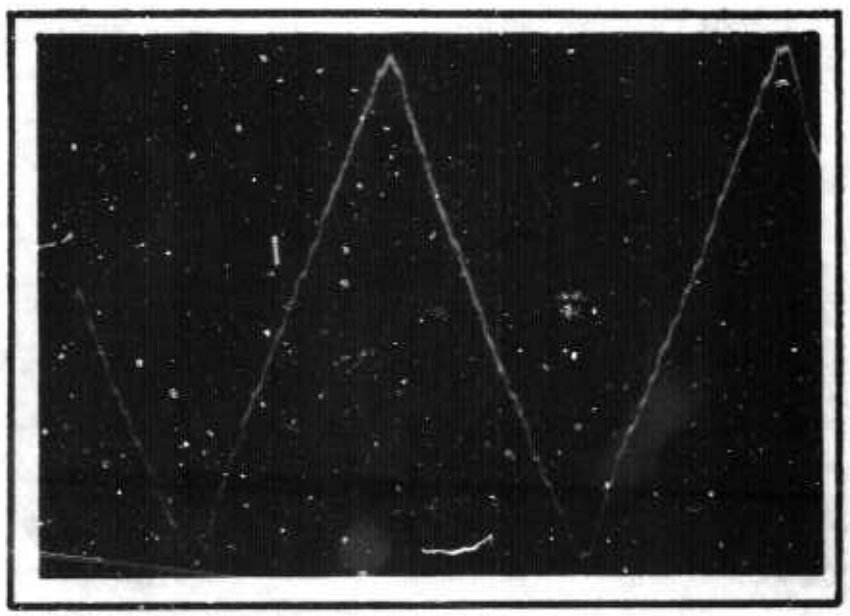

0.1 sec/cm 2 v/cm
Figure 13. Triangle Scan, 2 Hz

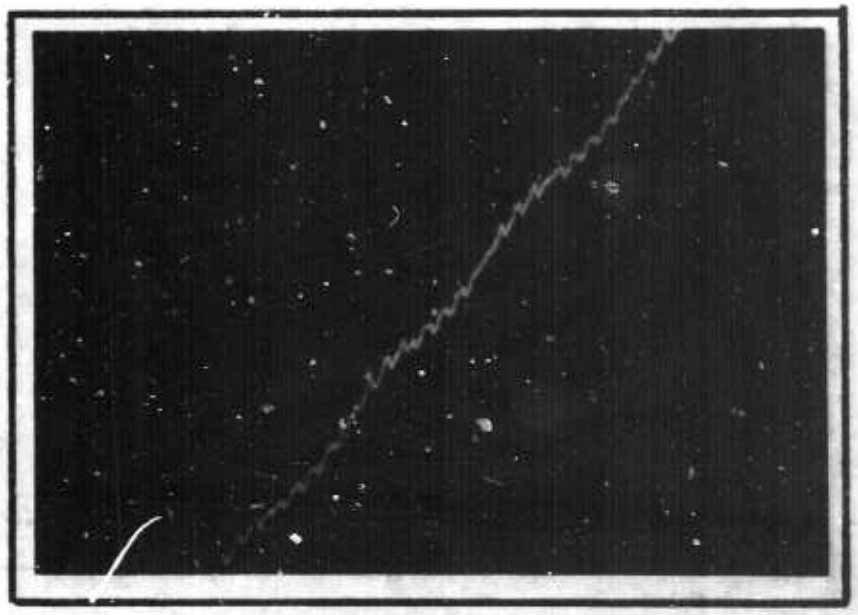

10 msec/cm 0.2 v/cm
Figure 14. Expanded Trace of Fig. 12

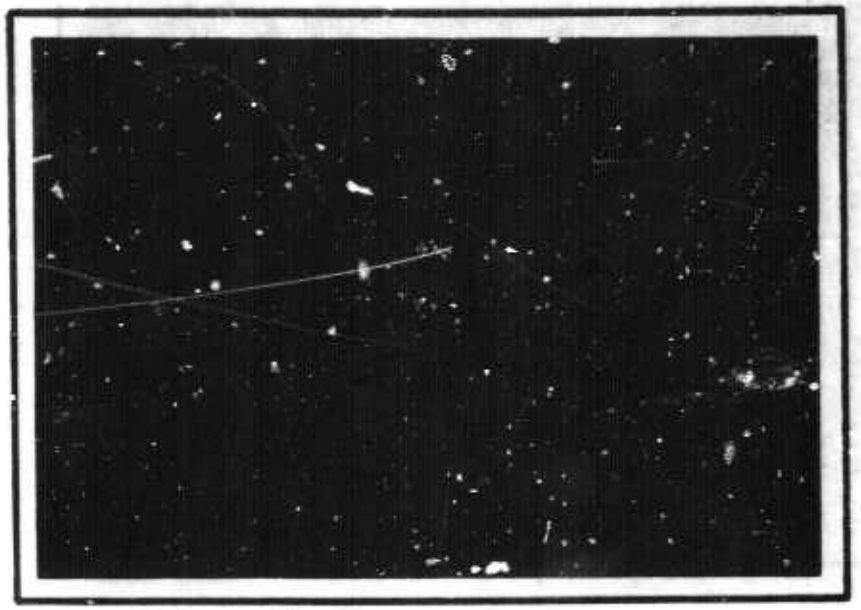

0.2 sec/cm 2 v/cm
Figure 15. Sine Scan, $\frac{1}{2}$ Hz

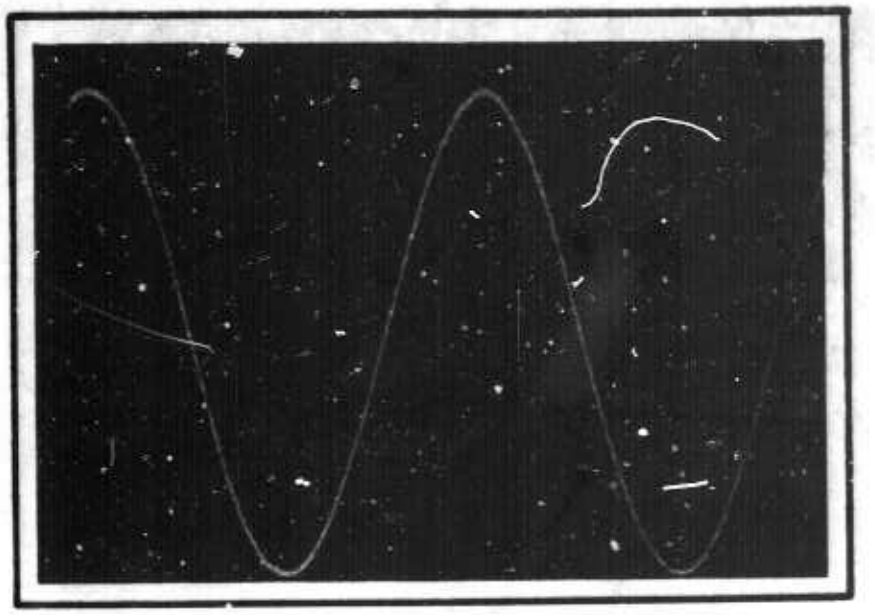

0.2 sec/cm 2 v/cm
Figure 16. Sine Scan, 1 Hz

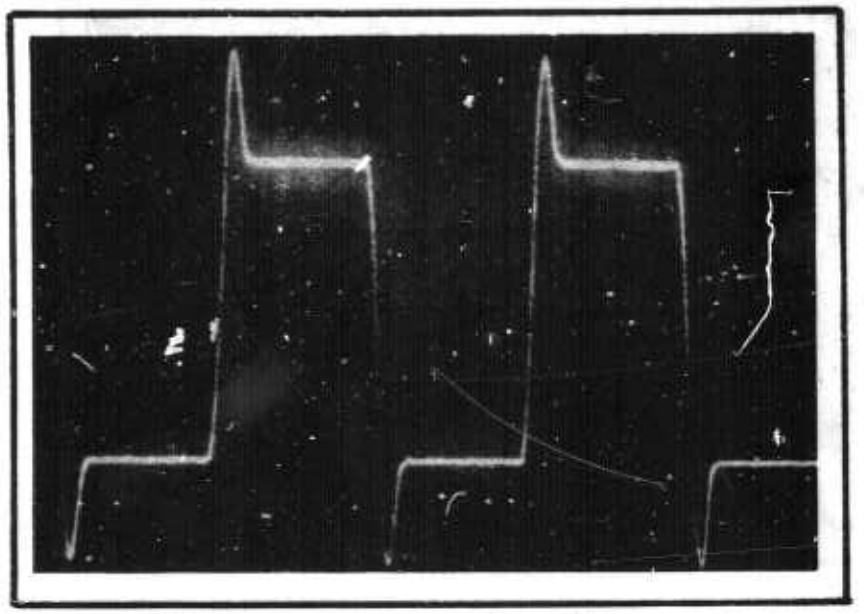

0.5 sec/cm 2 v/cm
Figure 17. Square Scan, $\frac{1}{2}$ Hz

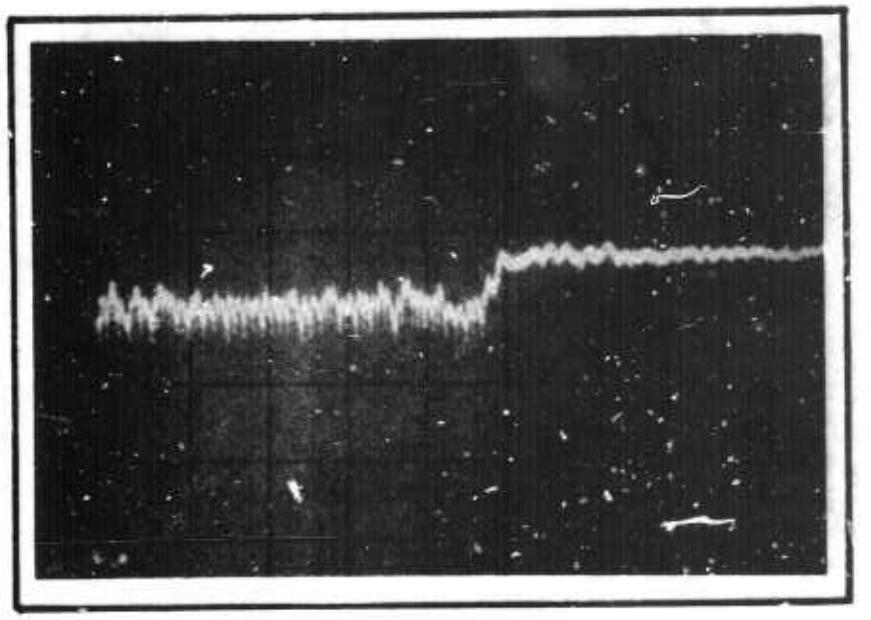

0.5 sec/cm 0.1 v/cm
Figure 18. Loaded Lock Mode

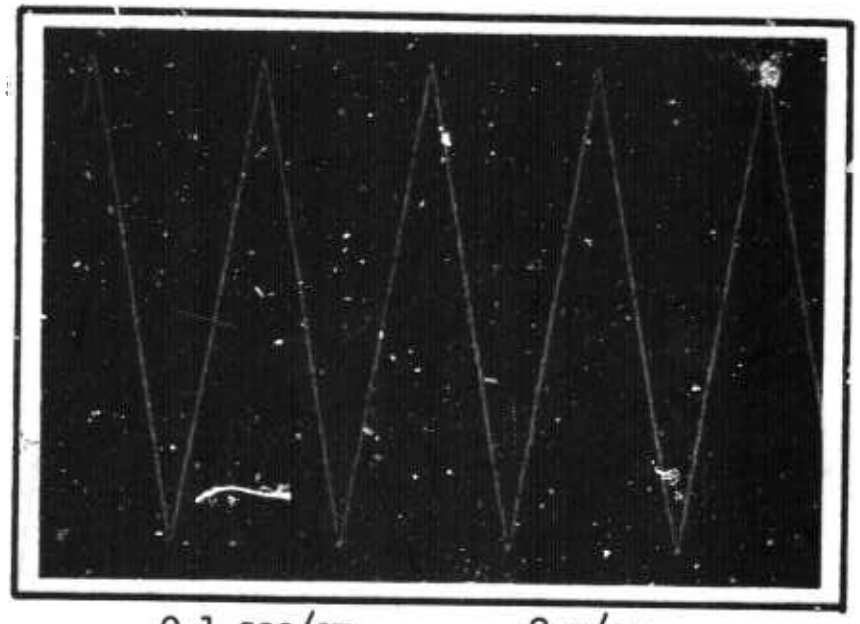

0.1 sec/cm 2 v/cm
Figure 19. Ballistic Scan, 4.6 Hz

0.1 sec/cm 1 v/cm
Figure 20. Ballistic Scan, 10 Hz

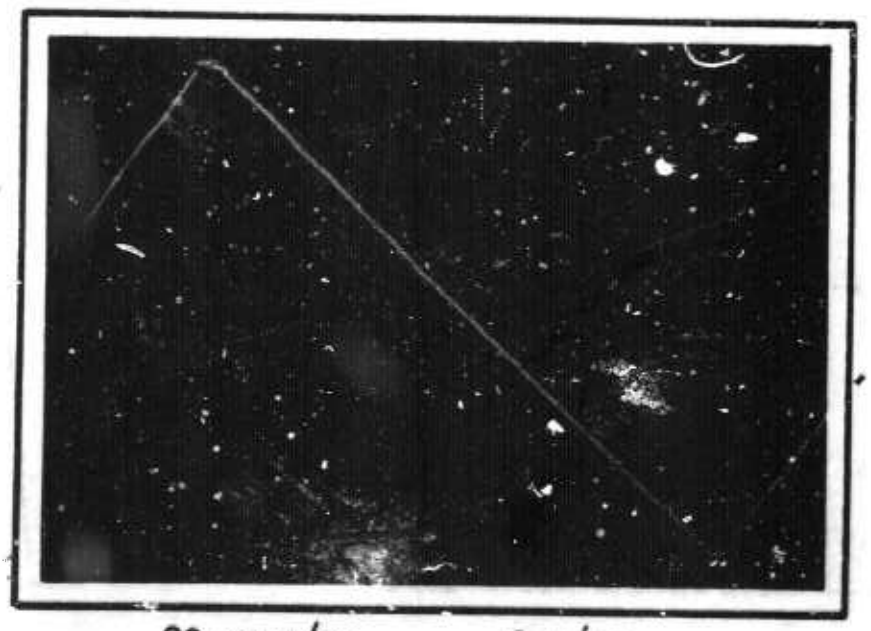

20 msec/cm 2 v/cm
Figure 21. Ballistic Scan, 3.7 Hz

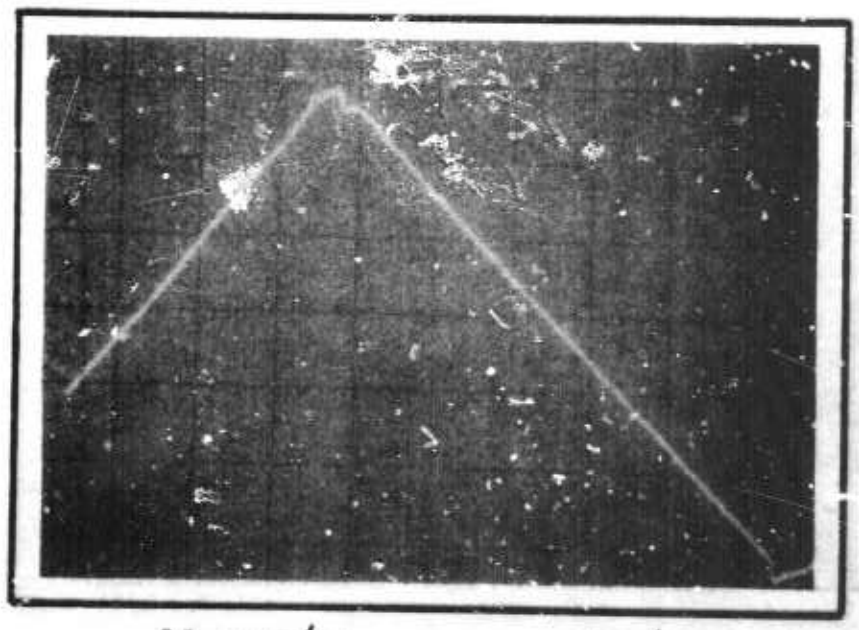

10 msec/cm 1 v/cm
Figure 22. Expansion of Fig. 20

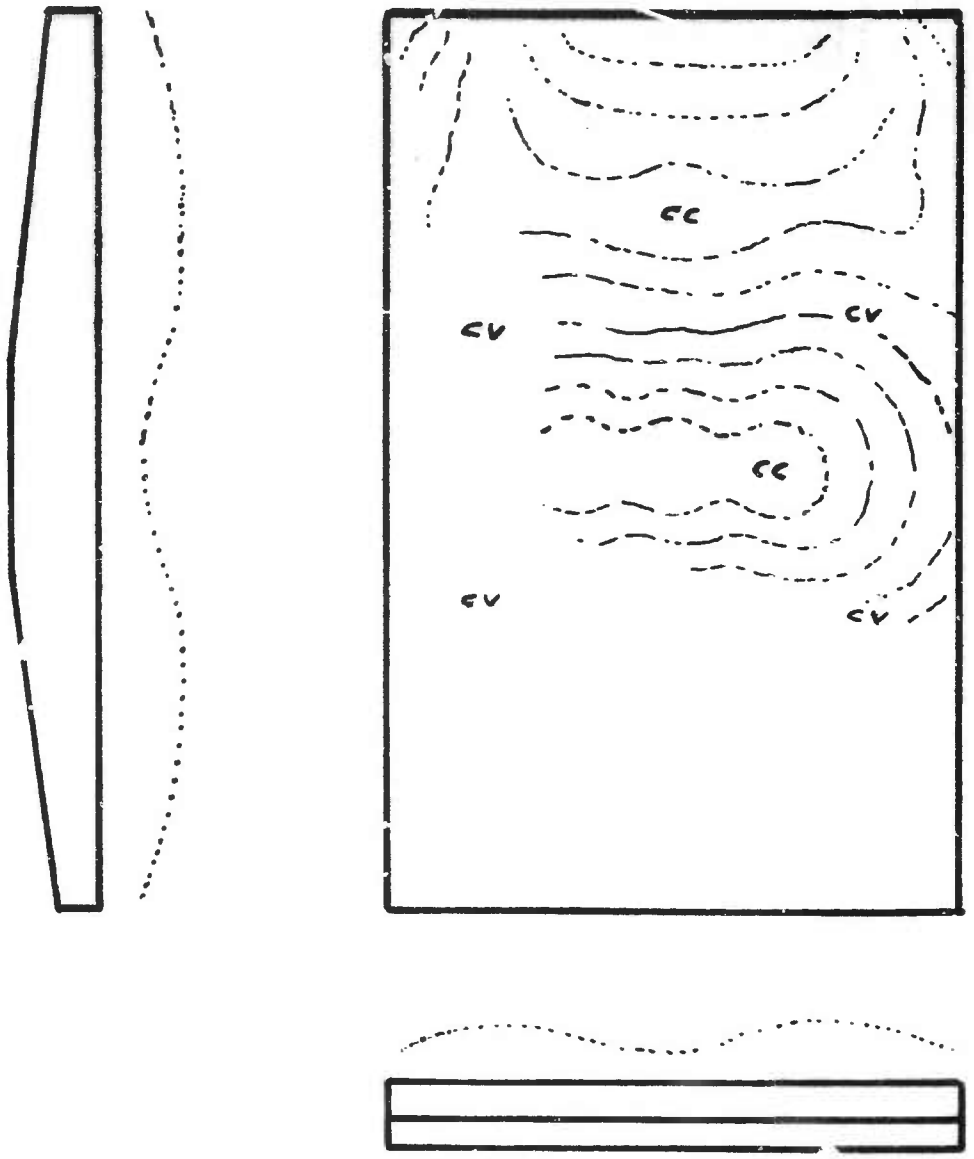

a) 4 fringes Hg per 6 inches, before
   3 " " " 6 " after
b) 6 " " " 6 " before
   4 " " " 6 " after

Figure 25. Surface Test

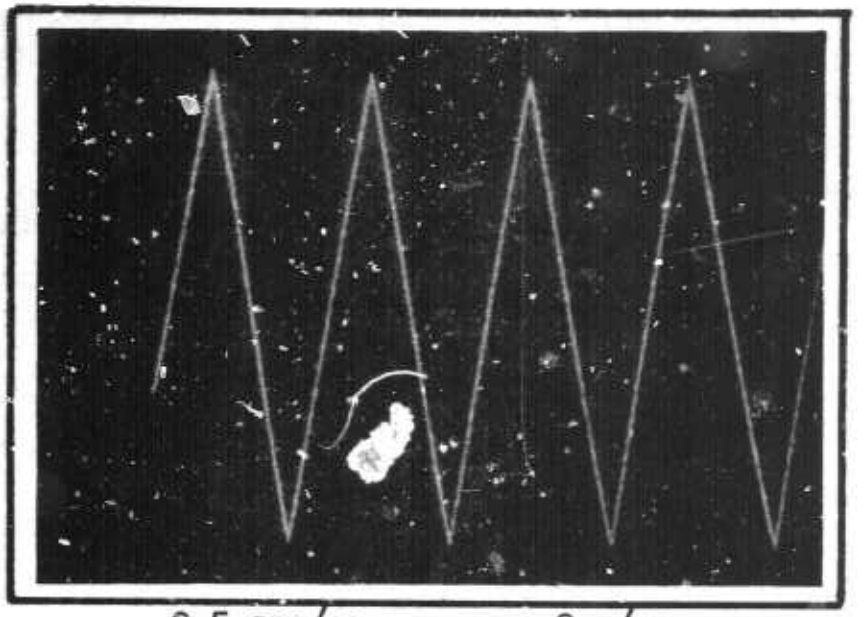

0.5 sec/cm 2 v/cm

Figure 23. Ballistic Scan, 1 Hz

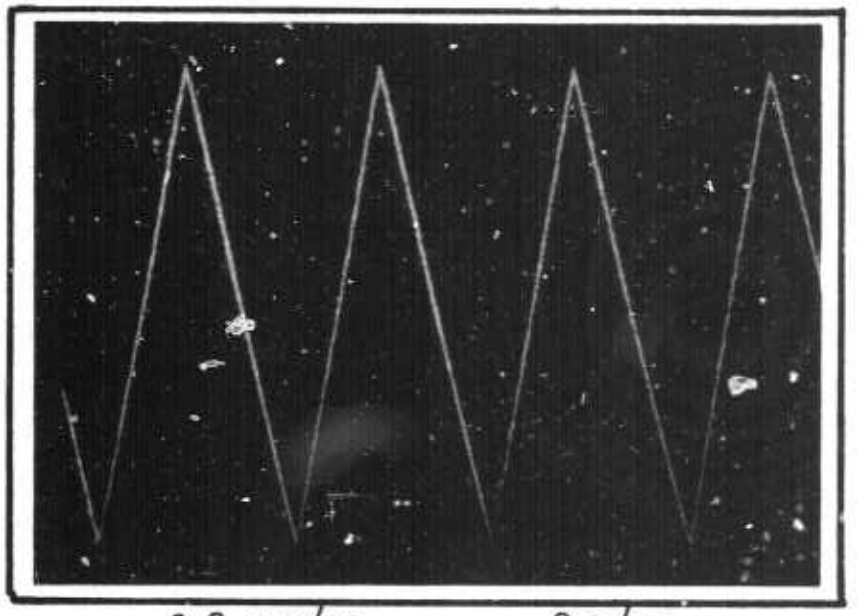

0.2 sec/cm 2 v/cm

Figure 24. Ballistic Scan, 2 Hz

VI. DEMONSTRATION OF FEASIBILITY

Using a single mirror feasibility demonstration model, feasibility has been demonstrated and 100 percent proven for the development of a two-mirror scanner generating a 3 deg by 3 deg raster field with linear scan at 0 to 10 Hz scan rate.

Objective	Actually Achieved	Feasibility Proven
Analog position pickoff with $\frac{1}{2}$ mrad resolution over 1.5 deg mirror angle	Yes	Yes
Azimuth rates 0 to 10 Hz over 0 to 1.5 deg mirror angle	to 10 Hz ballistic over 0.75 deg. $\frac{1}{2}$ to 5 Hz ballistic over 1.5 deg. 0 to 2 Hz slaved over 1.5 deg.	Yes
Elevation rate 0 to 3 Hz 0 to 1.5 deg. mirror angle	Yes	Yes
3 deg×3 deg field angle of raster	3 deg field with one mirror	Yes
Minimum turn-around time at field boundaries	5 msec at 10 Hz	Yes
Equal observation times per scan resolution element (1 mrad field)	Yes	Yes
Mirror remotely positionable to any angular resolution element	Yes	Yes
Scan linearity within one resolution element (1 mrad field)	Yes	Yes
Mirror flatness to 0.1λ at 10 microns	0.16λ	Yes
20 cm clear aperture at 45 deg.	Yes	Yes

APPENDIX I

Commentary

Concerning 10 cps at 1.5 deg Useful Ballistic Scan

From the oscillograms of Figures 19 and 20 where we achieve about 5 Hz at full scan amplitude, or 10 Hz at about half amplitude, it is apparent that an approximately doubled drive current in this model will provide full amplitude of ballistic scan at 10 Hz and with an extra deck of magnets would provide nearly 20 Hz at full scan. Even then, we are allowed still more current, being limited only by coil heating and resultant mirror distortion. This limitation should be far below the value which might aberrate the poling of the magnets. Thus, while we can now pass 6 amperes through the torquers, about 12 are actually needed.

During initial stages of the scanner design, the torquing coils were estimated at about 4 ohms resistance. Then the electronics were developed and checked out with a 4 ohm, 500μh coil as a dummy load. Meanwhile, a separate driver stage was planned for the counterweight torquer so that this and the mirror torquer could be given optimized currents. The extra drive stage was finally cancelled, since by the time the counterweight torquer was in design, it was found we could use about the same current as for the mirror torquer, and for simplification, a decision was made to operate these torquers in series. As it turned out, the mirror torquer finally came to 6 ohms and the two counterweight torquers to 2 ohms, giving twice the anticipated load for use on the mirror torquer drive transistors. By finding a higher voltage, high current supply we could have boosted the output only a little, quickly approaching the voltage rating of the drive transistors (60V). Program limitations prevent this and other modifications from being made at this time.

While shortage of driver current in the mirror has been mentioned in the test results, the electronics itself is in no sense current limited, but at the moment voltage limited. By incorporation of higher voltage power transistors with associated modifications, full amplitude at 10 Hz

(design goal) can surely be achieved. Since this is a feasibility demonstration program, we consider that we have adequately demonstrated feasibility on this item.

Another means of increasing energy of the scan drive pulses to improve amplitude at higher scan frequencies is to increase pulse duration. However, this increases scan stop distance, requiring scan reversal to be initiated at lower amplitudes to avoid hitting the mechanical limit stops. While having some merit, this approach was only briefly pursued.

Concerning Mirror Vibration

In some of the oscillograms we note a modulation suggesting vibration of the mirror. Testing dynamic flatness (flexural displacements and surface acoustic modes) of the mirror was not within the scope of the program. However, the scanner was designed in a manner at least incorporating most of the principles contributing to low vibration, although not doing complete justice to these principles because of program limitations.

For example, there was time only for a hurried check of the gap flux density of the distributed torquer magnets. Turning to Figure 1, seven magnets are observed to the right of the pivot axis. There are 14 such sets of 7. Each set was magnetized in groups of 2, 3, and 2, and temporarily assembled as one set, with the Alnico pieces picked at random from the supply that had been ground to size. Finally, each set was strapped to a test bar having ridges to provide the desired gapping, and gap flux density was measured by noting force on a current carrying conductor in the gap.

At that time it was the intention to remagnetize and redistribute the magnets among the sets until further gap tests indicated achievement of a uniform flux distribution among like gaps of the 14 sets, and of course, achievement of ratios of flux density among the gaps of each set approaching the design values. However, that effort was never begun; the magnet sets were finally employed in the scanner as initially assembled, with the exception that those sets having exceptionally strong (or weak) magnets were not embodied in the scanner side by side, but were separated. Considerable effort will be required in any future attempt to assemble a moderately idealized magnet array.

A test was made on an aluminum mirror, where by drilling of weight reducing holes it was found that weight could be reduced by about a third without impairing the quality of the repolished surface, although of course the overall stiffness was reduced. It is to be expected that the scanner mirror can be redesigned with less mass and yet maintain adequate overall stiffness (distributed torquing does not demand substantial stiffness). This will contribute to higher scan rates.

The mass reducing holes can be filled with acoustic damping material (such as polyisobutylene rubber) to achieve rapid damping of vibration induced by the torquing pulse. While absorption is typically difficult at low acoustic frequencies, the primary problem is that of coupling the sound to the absorber. By use of a myriad of damping wells distributed throughout the mirror, the acoustic impedance mismatch between the metal and the

absorber will be tempered by the innumerable incidences of sound wavefronts on the absorbers, and significant damping should result.

The oscillograms have indicated that at the pickoff position a flexural vibration exists. This is sufficiently small in terms of the smoothness of scan we wish to see. However, in terms of maintaining a mirror flatness of one tenth wave on a dynamic basis, we have no knowledge of the effect of the vibration. A mirror dynamic flatness test program can be approached in a number of ways. One could begin by exploring the mirror surface with a miniature accelerometer. One could arrange an interferometer illuminated by a pulsed ruby laser as the scanner passes through parallelism with a fixed mirror. Or, holographic techniques could be employed.

Concerning Scan Linearity

During operation of the servo control mode, suitably compensated electronics (rate, and integral control, etc.) can hold the scan as closely as desired to the function generator waveform. This requires a quality waveform. Also required is a highly linear position pickoff of good frequency capability. The pickoff employed on the mirror has demonstrated a linearity around one percent of full travel even though having an arc motion. The circuitry provides a frequency response of 6 kHz at 3 db down. Uniformity of flux density throughout the gap of any given pole pair is not particularly significant except in terms of vibration performance. For the servo mode, the overall current will be adjusted to the value required to keep the instantaneous position error small, and for these low frequencies of scan, vibration is not significantly excited. More specifically, if excited, it will be at the frequency of control which in this model is about 500 Hz but which can be made 5 or 10 kHz, where the induced vibration amplitude goes down with rise in frequency and where it is also damped more readily. Other approaches to servo control can eliminate use of the clock rate, and in this manner reduce vibration input.

In the ballistic mode, scan reversal might be commanded to occur at a different amplitude of scan at one time than at another, thus requiring use of the torquer in a new position in the magnet gaps, where the field strength is somewhat different. However, since the pulse is very short and displacement small during pulse delivery (4 mils at 6-inch radius for a 5 msec pulse at 10 Hz), linearity of motion is not a function of torquing but of absence of spring rate and damping influences during the ballistic trajectory. Linearity must be the same at all points on the mirror, and this merges with the realm of minimizing flexural vibration and acoustic mode patterns, as discussed above.

Air damping is not considered significant at 10 cps or even at 25 Hz, although drafts of air may disturb the ballistic scan. If the latter condition is discovered and cannot be shielded, then we would suggest mixing servo control with ballistic operation, where the ballistic impulse supplies peak demands and the servo supplies only a feeble torquing to improve linearity point by point.

Another source of damping may be accumulation of ferrous particles in the magnet gaps, forming bridges that drag upon the moving coil. With care, this can be totally avoided.

Concerning Ballistic Scan Walkoff

At the higher ballistic scan frequencies, it has been found substantially impossible to manually maintain a proper ratio of CW and CCW torquing current strengths to prevent scan walkoff. Walkoff appears in the form of differing launch rates of CW and CCW scans with divergence occuring to the point of scan cessation. If the CW scan is too slow, as it approaches the scan reversal position, then the CCW launch velocity will be extra large. The following CW pulse therefore tends to be used up to stop the CCW scan, with insufficient strength remaining to effect a CW launch velocity as great as the previous CW launch, which, relatively, was evidently already weak, perhaps partly from an imperfect start pulse. Thus, walkoff is self-amplifying.

The solution can be provided by an electronic servo to adjust relative mirror launch rates. Program limitations have not permitted development of such a servo; but for actual use of the model and not merely demonstration of feasibility, as has been accomplished, this servo is imperative.

One approach is to time each scan line between reversals and adjust the relative pulse strengths to maintain CW and CCW scans of equal duration. If desired, rates can be monitored and integrated during each scan line, employing the torquing coil as a rate pickoff, and thus allowing correction on the next torquing pulse. If a combination of servo and ballistic operation were employed, rate sensing and servo correction could be time shared during the initial phase of each scan to correct that scan, and not await correction of the next scan. However, this refinement will probably be found quite unnecessary, but it is available as a backup to the simpler approach.

Raster Step Function

In a two-mirror scanner with one mirror providing a raster scan and the other a step motion between scan lines, it is significant to demonstrate feasibility of the step operation as well as the scan operation.

Scan operation of the present model has been demonstrated at approximately 5 Hz for 1.5 deg and at 10 Hz for about 3/4 deg, with feasibility of reaching 1.5 deg clearly explained. Now that a 10 Hz scanner of useful duty cycle of 0.9 over 1.5 deg has been shown feasible, we shall show that the step function must in turn be feasible. The 10 Hz scan will take 0.045 sec, giving a velocity of

$$\omega = \frac{\Delta\theta}{\Delta t} = \frac{(1.5 \text{ deg})\pi}{180 \text{ deg}} \quad \frac{1}{0.045 \text{ sec}} = 0.582 \text{ rad/sec}$$

For the 5 msec scan reverse pulse, only 2.5 msec is used for acceleration or for deceleration.

Thus,

$$\alpha = \frac{\omega}{t} = \frac{0.582 \text{ rad/sec}}{2.5\text{X}10^{-3}\text{sec}} = 233 \text{ rad/sec}^2.$$

The step motion is taken as one resolution element of scan, which is 1 mrad field angle or $\frac{1}{2}$ mrad mirror angle. In stepping, there is an acceleration through $\frac{1}{4}$ mrad for 2.5 msec and a deceleration of like angle and time. Thus,

$$\theta = \tfrac{1}{2}\alpha t^2$$

$$\alpha = \frac{2\theta}{t^2} = \frac{2(0.25\text{X}10^{-3}\text{rad})}{(2.5\text{X}10^{-3}\text{sec})^2} = 80 \text{ rad/sec}^2$$

Since torques are proportional to accelerations, we have for a step current I and scan current I^* at 10 Hz,

$$I = \frac{80}{233} I^* = 0.35 I^*$$

Thus, the required current is about one third of the value I^* for scan reversal at 10 Hz, and is also less than the current $0.5I^*$ required for scan reversal at 5 Hz and 1.5 deg as already achieved. Feasibility of stepping (in 5 msec) is proven.

The scan pulse of 5 msec is equivalent to a frequency of 100 Hz. Since the step pulse is a doublet of the same duration, it has a frequency of 200 Hz. Thus,

$$2\pi FL = 2\pi\ 200(600\text{X}10^{-6}\text{henry}) = 0.75 \text{ ohm}$$

This is negligible compared with 6 ohms resistance of the coil and will not significantly increase coil impedance. Thus, only a low doublet current is needed, and it can easily be put through the distributed torquer. Hence, feasibility of the mirror stepping action remains demonstrated.

Variable Amplitude and Position

It is clear that the servo mode of scan can be extended through at least 2 Hz at a displacement of 1.5 deg on the mirror. Smaller displacements down to 0 amplitude are clearly demonstrated. Slew of the lock mode, and hence ability to set the servo mode reference off center of the 1.5 deg scan is evident. Thus, the servo mode can operate through any angular range about any reference within boundaries of the 1.5 deg design limits.

The ballistic mode scan limits are governed by threshold settings of the Schmidt circuit triggers. Although these cannot reach zero voltage, other circuitry, such as introduction of biases in the position pickoff voltage, can cause the Schmidt triggers to trip near zero voltage on the pickoff to bring CW and CCW scan pulses adjacent each other on a time scale and at any angle within the 1.5 deg scan range. There are many ways to set threshold from 0 to 1.5 deg. Thus, ballistic operation is feasible through any angular range about any reference within boundaries of the 1.5 deg design limits.

Ballistic Scan Stop Capability

The ballistic scan motion in the feasibility model is stopped by a pulse of 5 msec duration having half the height of the scan reversal pulse. This duration was selected for a 0.9 duty cycle at 10 cps, and can be lengthened if it is desired to reduce a current level. At a scan velocity of 0.582 rad/sec corresponding to 10 Hz at 1.5 deg useful angle,

$$\theta = \omega t = \left(\frac{.582 \text{ rad}}{2 \text{ sec}}\right)(.005 \text{ sec}) = 1.46 \times 10^{-3} \text{rad}$$

To stop within 1 mrad resolution element of fixed angle, or $\frac{1}{2}$ mrad mirror angle, would require 0.00146/.0005 = 2.9 times the half current pulse or $1\frac{1}{2}$ times the current of the scan reversal pulse. For a single pulse, overheating will surely not be a consideration. This pulse can certainly be delivered with modified electronics. Hence, the scan can be stopped within one resolution element of scan if desired.

APPENDIX II

Design Approach to Distributed Torquing

As a first step, the mirror is divided into a number of imaginary segments to either side of the pivot axis. About this axis, centers of percussion and moments of inertia of the segments are found. Torquing requirements for all segments are determined, and coils and coil support pylons are roughly designed. With these loads on the mirror sections, new centers of percussion and moments of inertia are calculated. These inertias are then plotted as a function of radius arm, and the curve is examined for smoothness.

Peaks or valleys on the curve represent greater than necessary differentials in inertias and hence in torques between adjacent segments. Since the coils have a small and integral number of conductors and all coils are in series, the currents per coil will not be optimal. Because of this and mechanical tolerances preventing each coil force from really being applied at the center of percussion, unbalance torques exist between segments of mirror. In addition, each segment is merely a block that really should be driven at all points, but which in practice can only be driven at the pylon points for the coil, resulting in bending moments within each segment. Therefore, the attempt at distributed torquing is bound to fall short of its goal.

However, we must minimize obvious torque nonuniformities to reduce bending moments between the segments into which the mirror is imagined to be divided. While a suitable mirror stiffness will easily prevent these moments, or short-arm force couples, from directly distorting the mirror surface, nonetheless, pulse torquing can in this manner induce vibration in the mirror, which may set up resonances and mode patterns on the surface. In addition to these problems, optimum torquing efficiency is desired, which at least requires that there are not too many flux weakening air gaps in the magnetic circuit, and yet that there are not so few gaps that torquing becomes too coarsely distributed. Thus, models of the magnetic circuit

must be made to see if we can really obtain the gap fluxes and hence torquing capability we have thus far assumed in the design. These models must be determined in the laboratory, not analytically, since leakage fluxes are unknown and can be quite enormous.

After evaluating and redesigning the magnetic circuit, the above calculations on moments of inertia and centers of percussion must be dumped, and the mirror must be redivided into new imaginary segments, which is not merely a matter of adjusting segment length and position but also of adjusting the mirror thickness and taper. Then, new calculations are made and updated magnetic circuits are tested. The design approach becomes one of successive approximations until coarseness of torquing due to a series current in a discrete number of conductors per air gap remains the greatest error in achieving uniformly distributed torquing for the number of torquing stations available, where the number of stations is optimized within limitations of the magnetic circuit, and provided that a uniform magnetic circuit is actually employed.

Unfortunately, the above optimization is quite defeated if the flux density at all parts of the magnetic circuit is not as uniform as we would like it to be. The actual magnitude of flux density is not too important, since this can be accommodated by optimized ampere turns in the coil, but we would like assurance that throughout the length of each torquing coil the same flux density is observed at all of the magnetic gaps. This condition, while not attempted in the model, could be achieved by selecting the magnets and by magnetizing them quite exactly, or by knocking down magnetization of the strongest to that of the weakest. So herein lies the greatest single source of error in achieving uniformity of torquing, unless exorbitant effort is employed in building the magnetic circuit.

A series connection of the torquing coils is required for any given source of drive current in order to prevent damping of the mirror ballistic trajectory due to currents resulting from the counter emf. Thus, individual coil currents cannot be resistor trimmed. Neither can coils be put in parallel or series parallel arrangements for adjustment of current in each

coil, since nonuniformities of the magnetic circuit will cause unequal induced emf's which will in turn cause circulating currents even between identical coils. Since current enters at one flexural pivot and exits at the other, one drive electronic package must serve the total mirror. Complex multiple flexures are, of course, possible in order to have n drive outputs for n coils but this is not practical. Clearly, each drive package must have a very low impedance during pulse delivery and a very high impedance between pulse deliveries.

While coils of many turns of fine wire could reduce the ampere turns error for a series current, inductance and resistance could rise. Difficulty of fabrication of the coils and of self-support over substantial spans would also increase. Thus, the conductors per gap are relatively few and range from 7 to 14 turns of 24-gage wire, giving a series resistance of 6 ohms and inductance of 0.6 millihenries for the mirror torquer.

Since each coil structure of the distributed torquer must be rotated through the same angle as the mirror segment it drives, a bending moment in that segment, and probably over a greater region, is generated to accelerate the coil in rotation. This moment can be eliminated in a scanner having a double deck of magnets by slightly tilting each flux gap out of the plane passing through the center of percussion of the associated mirror segment. With opposite tilts of small amount on the top and bottom deck of magnets via greater or less sloping of the magnet faces defining the gap, thrust vectors of the top and bottom conductor sets can have an angle between them which will directly provide a rotational component to the gross coil, thus eliminating need for the mirror to supply a force couple to rotate the coil via the pylons. This will further reduce vibration inputs to the mirror by a small amount.

APPENDIX III

Concerning the Magnetic Structure

A number of experiments were performed on magnetic structures, which for a horizontally disposed mirror surface consisted of a forest of tall, vertical bar magnets terminated in rectangular blocks of iron with vertical pole faces. This arrangement would permit a box-like coil to be placed around alternate poles so that one coil side would lie in the gap between each set of pole faces. Thus, going from one end of the mirror to the other, the gap flux would be horizontal and would be found to alternate in direction from gap to gap.

Because of very high leakage flux between the vertical bar magnets, gap flux between pole pieces was weak. Leaving the pole arrangement intact but eliminating every other magnet to reduce direct leakage between magnets served only to further reduce gap flux. In either arrangement, gap flux was quite sensitive to changes in pole spacing.

In these experiments a variety of magnet sizes were used, ranging between tall, short, thick, and thin, and with poor results. The forest of vertical magnets terminated in horizontal pole pieces and was abandoned in favor of directly replacing the soft pole pieces with hard magnet material, and having no other magnets. Thus, the best magnetic structure became one in which short horizontally disposed bar magnets were spaced sufficiently to form air gaps to receive torquing coils.

Gap flux in the latter arrangement was found superior, in spite of a much lower total volume of magnet material. In addition, the flux density (about 2 kilogauss in an 80 mil gap) was found relatively insensitive to variations in gap width. Furthermore, elimination of soft poles presumably reduces inductance of the torquing coils since the ampere turns are insufficient to change the pole flux.

However, in going from one end of the mirror to the other, all gap fluxes are of the same polarity, so all conductor currents must be in the same direction; each set of conductors must be returned outside of the gap. Thus, instead of box coils where both coil sides are useful, planar coils are now required. These are more amenable to tilting off the vertical. These coils, and their tilted attitudes, may be observed in the photograph of Figure 5. The array of magnets (Figures 3, 4) is positioned between the set of conductors nearest the mirror.

It is interesting to note that future rework of this scanner model could provide for an extra deck of magnets between the outer portions of the planar coils, nearly doubling the mirror torquing. In addition, since this second deck of magnets would be positioned with opposite polarity to the first set, a closed magnetic circuit would be possible, offering a slight improvement in flux at the ends of the array.

UNCLASSIFIED
Security Classification

DOCUMENT CONTROL DATA - R & D

(Security classification of title, body of abstract and indexing annotation must be entered when the overall report is classified)

1. ORIGINATING ACTIVITY *(Corporate author)*
North American Rockwell Corporation
Autonetics Division
3370 Miraloma Avenue
Anaheim, Calif, 92803

2a. REPORT SECURITY CLASSIFICATION
Unclassified

2b. GROUP

3. REPORT TITLE

10.6 MICRON OPTICAL SCANNER

4. DESCRIPTIVE NOTES *(Type of report and inclusive dates)*
Final Report May 1969 to February 1970

5. AUTHOR(S) *(First name, middle initial, last name)*

R. L. Treuthart

6. REPORT DATE	7a. TOTAL NO. OF PAGES	7b. NO. OF REFS
March 1970	47	0

8a. CONTRACT OR GRANT NO.	9a. ORIGINATOR'S REPORT NUMBER(S)
F30602-69-C-0136 b. XXXXXXXXX ARPA Order No. 1279 c. d.	C70 231/501 9b. OTHER REPORT NO(S) *(Any other numbers that may be assigned this report)* RADC-TR-70-48

10. DISTRIBUTION STATEMENT
This document is subject to special export controls and each transmittal to foreign governments or foreign nationals may be made only with prior approval of RADC (EMATA), GAFB, NY 13440.

11. SUPPLEMENTARY NOTES	12. SPONSORING MILITARY ACTIVITY
Monitored by Robert F. Ogrodnik AC 315 330-4305 RADC (EMATA), GAFB, NY 13440	Advanced Research Projects Agency Washington, DC 20301

13. ABSTRACT

A ballistic optical scanner stopped and reversed by a current impulse at each extreme of scan motion, and accomplishing each direction of scan motion via momentum from the drive impulses has been shown to be a feasible means of achieving equal observation times per scan resolution element. Operation from 0 to ± 3/4 deg mirror angle from 2 to 10 Hz has been shown to be feasible. Operation through this angle from 0 to 2 Hz in a servo mode, with the scanner displacement slaved to a triangular (or other) voltage waveform has also been shown feasible. This scanner, of 20 cm clear aperture at 45 deg incidence, has a versatility of control enabling a ballistic search mode to be stopped anywhere within one resolution element of scan (1/2 mrad mirror angle), where the position may be locked, or where target tracking may then be accomplished by the servo mode of control. The use of two independent mirrors will permit a raster scan having a 3 deg by 3 deg field angle.

DD FORM 1 NOV 68 1473

UNCLASSIFIED
Security Classification

14. KEY WORDS	LINK A		LINK B		LINK C	
	ROLE	WT	ROLE	WT	ROLE	WT
Optical Beam Scanner for [illegible] Microns						
Ballistic Scanner						
Impulse Torquer Scan Cont[illegible]						
Raster Scan Pattern						